

**Tetrahydro-2-naphthyl and 2-indanyl triazolopyrimidines  
targeting *Plasmodium falciparum* dihydroorotate  
dehydrogenase display potent and selective antimalarial activity**

Sreekanth Kokkonda, Xiaoyi Deng, Karen L. White, Jose M. Coterón, Maria Marco, Laura de las Heras, John White, Farah El Mazouni, Diana R Tomchick, Krishne Manjаланagara, Kakali Rani Rudra, Gong Chen, Julia Morizzi, Eileen Ryan, Werner Kaminsky, Didier Leroy, Maria Santos Martínez-Martínez, Maria Belen Jimenez Diaz, Santiago Ferrer Bazaga, Iñigo Angulo-Barturen, David Waterson, Jeremy N. Burrows, Dave Matthews, Susan A. Charman, Margaret A. Phillips, and Pradipsinh K Rathod

*J. Med. Chem.*, **Just Accepted Manuscript** • DOI: 10.1021/acs.jmedchem.6b00275 • Publication Date (Web): 29 Apr 2016

Downloaded from <http://pubs.acs.org> on April 30, 2016

**Just Accepted**

“Just Accepted” manuscripts have been peer-reviewed and accepted for publication. They are posted online prior to technical editing, formatting for publication and author proofing. The American Chemical Society provides “Just Accepted” as a free service to the research community to expedite the dissemination of scientific material as soon as possible after acceptance. “Just Accepted” manuscripts appear in full in PDF format accompanied by an HTML abstract. “Just Accepted” manuscripts have been fully peer reviewed, but should not be considered the official version of record. They are accessible to all readers and citable by the Digital Object Identifier (DOI®). “Just Accepted” is an optional service offered to authors. Therefore, the “Just Accepted” Web site may not include all articles that will be published in the journal. After a manuscript is technically edited and formatted, it will be removed from the “Just Accepted” Web site and published as an ASAP article. Note that technical editing may introduce minor changes to the manuscript text and/or graphics which could affect content, and all legal disclaimers and ethical guidelines that apply to the journal pertain. ACS cannot be held responsible for errors or consequences arising from the use of information contained in these “Just Accepted” manuscripts.

SCHOLARONE™  
Manuscripts

1  
2  
3  
4  
5  
6  
7  
8  
9  
10  
11  
12  
13  
14  
15  
16  
17  
18  
19  
20  
21  
22  
23  
24  
25  
26  
27  
28  
29  
30  
31  
32  
33  
34  
35  
36  
37  
38  
39  
40  
41  
42  
43  
44  
45  
46  
47  
48  
49  
50  
51  
52  
53  
54  
55  
56  
57  
58  
59  
60

**Tetrahydro-2-naphthyl and 2-indanyl triazolopyrimidines targeting*****Plasmodium falciparum* dihydroorotate dehydrogenase display potent and selective  
antimalarial activity**

Sreekanth Kokkonda<sup>1</sup>, Xiaoyi Deng<sup>2</sup>, Karen L. White<sup>3</sup>, Jose M. Coteron<sup>4</sup>, Maria Marco<sup>4</sup>, Laura de las Heras<sup>4</sup>, John White<sup>1</sup>, Farah El Mazouni<sup>2</sup>, Diana R. Tomchick<sup>5</sup>, Krishne Manjаланagara<sup>6</sup>, Kakali Rani Rudra<sup>6</sup>, Gong Chen<sup>3</sup>, Julia Morizzi<sup>3</sup>, Eileen Ryan<sup>3</sup>, Werner Kaminsky<sup>1</sup>, Didier Leroy<sup>7</sup>, María Santos Martínez-Martínez<sup>4</sup>, Maria Belen Jimenez-Diaz<sup>4</sup>, Santiago Ferrer Bazaga<sup>4</sup>, Iñigo Angulo-Barturen<sup>4</sup>, David Waterson<sup>7</sup>, Jeremy N. Burrows<sup>7</sup>, Dave Matthews<sup>7</sup>, Susan A. Charman<sup>3</sup>, Margaret A. Phillips<sup>2\*</sup> and Pradipsinh K. Rathod<sup>1\*</sup>

<sup>1</sup>Departments of Chemistry and Global Health, University of Washington, Seattle, WA 98195;

<sup>2</sup>Departments of Pharmacology and <sup>5</sup>Biophysics, University of Texas Southwestern Medical Center at Dallas, 6001 Forest Park Blvd, Dallas, Texas 75390-9041; <sup>3</sup>Centre for Drug Candidate Optimisation, Monash Institute of Pharmaceutical Sciences, Monash University, Parkville, VIC 3052, Australia, <sup>4</sup>GSK, Tres Cantos Medicines Development Campus, Severo Ochoa, Madrid, 28760 Spain, <sup>6</sup>Syngene International Ltd, Bangalore, India, 560 099; <sup>7</sup>Medicines for Malaria Venture, 1215 Geneva, Switzerland.

\*Authors to whom all correspondence should be addressed.

## Abstract

Malaria persists as one of the most devastating global infectious diseases. The pyrimidine biosynthetic enzyme dihydroorotate dehydrogenase (DHODH) has been identified as a new malaria drug target and a triazolopyrimidine-based DHODH inhibitor **1** (**DSM265**) is in clinical development. We sought to identify compounds with higher potency against *Plasmodium* DHODH while showing greater selectivity towards animal DHODHs. Herein we describe a series of novel triazolopyrimidines wherein the p-SF<sub>5</sub>-aniline was replaced with substituted 1,2,3,4-tetrahydro-2-naphthyl or 2-indanyl amines. These compounds showed strong species selectivity and several highly potent tetrahydro-2-naphthyl derivatives were identified. Compounds with halogen substitutions displayed sustained plasma levels after oral dosing in rodents leading to efficacy in the *P. falciparum* SCID mouse malaria model. These data suggest that tetrahydro-2-naphthyl derivatives have the potential to be efficacious for the treatment of malaria, but due to higher metabolic clearance than **1**, they most likely would need to be part of a multi-dose regimen.

## Introduction

Malaria is one of the most deadly infectious diseases in human history with 3.2 billion people in 97 countries at risk.<sup>1</sup> An estimated 444,000 deaths from malaria were reported by the WHO in 2015 and ~90% of these occurred in sub-Saharan Africa, mostly amongst children under the age of five. Human malaria, which is transmitted by the female Anopheles mosquito, can be caused by five species of *Plasmodia*, however *Plasmodium falciparum* and *Plasmodium vivax* are the most significant.<sup>2,3</sup> *P. falciparum* is dominant in Africa and accounts for most of the deaths, while *P. vivax* has a larger global distribution. To simplify treatment options it is desirable that new drugs be efficacious against all human infective species.<sup>4</sup> Malaria is a treatable disease and malarial control programs depend on drug therapy for treatment and chemoprevention, and on insecticides (including insecticide impregnated bed nets) to prevent transmission.<sup>2</sup> A large collection of drugs has been used for the treatment of malaria, but many of the most important compounds have been lost to drug resistance (e.g. chloroquine and pyrimethamine).<sup>4-6</sup> Artemisinin combination therapies (ACT) replaced older treatments, becoming highly effective, crucial tools in global efforts that have led to the decline in malaria deaths over the past decade. However, resistance to the artemisinin components (associated with Kelch13 propeller protein mutations<sup>7-9</sup>) has been found in Southeast Asia putting at risk malaria treatment programs. To combat drug resistance a significant effort is underway to identify new compounds that can be used for the treatment of malaria, with several new entities currently in clinical development.<sup>4, 5, 10</sup>

The triazolopyrimidine DSM265 (**1**) (Fig. 1) developed by our group is the first antimalarial agent that targets dihydroorotate dehydrogenase (DHODH) to reach clinical development, validating this target for the treatment of malaria.<sup>11, 12</sup> DHODH is a mitochondrial

1  
2  
3 enzyme that is required for the fourth step of de novo pyrimidine biosynthesis, catalyzing the  
4  
5 flavin-dependent oxidation of dihydroorotate to orotic acid with mitochondrially derived  
6  
7 coenzyme Q (CoQ) serving as a second substrate.<sup>13</sup> Pyrimidines are essential for both RNA and  
8  
9 DNA biosynthesis and because *Plasmodia* do not encode pyrimidine salvage enzymes, which are  
10  
11 found in humans and other organisms, the *de novo* pyrimidine pathway and DHODH are  
12  
13 essential to the parasite. We identified the triazolopyrimidine DHODH inhibitor series by a  
14  
15 target-based high throughput screen, and the initial lead DSM1 (**2**) (Fig. 1) was shown to  
16  
17 selectively inhibit *P. falciparum* DHODH and to kill parasites *in vitro* but it was ineffective *in*  
18  
19 *vivo* due to poor metabolic properties.<sup>14-16</sup> The series was subsequently optimized to improve its  
20  
21 *in vivo* properties resulting in the identification of DSM74 (**3**), which while metabolically stable  
22  
23 lacked potency.<sup>16</sup> X-ray structures of **2** and **3** bound to *Pf*DHODH were then used to guide the  
24  
25 medicinal chemistry program in the search for more potent analogs, resulting in the identification  
26  
27 of **1**.<sup>11, 12, 17</sup>  
28  
29  
30  
31  
32  
33  
34

35 While **1** has progressed successfully to Phase II clinical trials,<sup>4</sup> we sought to identify  
36  
37 potential backup compounds if unforeseen issues arise during its clinical development.  
38  
39 Importantly, **1** has potent activity on *Pf*DHODH and *P. falciparum* parasites *in vivo*, and its  
40  
41 pharmacokinetic properties support its use as a single dose treatment or once weekly  
42  
43 prophylactic.<sup>12</sup> However, while **1** has excellent selectivity against human DHODH and thus is  
44  
45 not expected to show on target activity in humans, it does have some activity against rodent  
46  
47 DHODHs that has complicated animal toxicity testing. We therefore sought to identify  
48  
49 compounds that have broad selectivity against all mammalian DHODHs, while if possible  
50  
51 identifying compounds with higher potency against *Pf*DHODH that could potentially reduce the  
52  
53 dose required for treatment. We describe herein a series of triazolopyrimidines where the SF<sub>5</sub>-  
54  
55  
56  
57  
58  
59  
60

1  
2  
3 aniline moiety of **1** has been replaced by either substituted 1,2,3,4-tetrahydro-2-naphthyl or 2-  
4 indanyl amines. Compounds from both series are inactive against a range of mammalian  
5  
6 DHODHs, while several of the identified tetrahydronaphthalenes are more potent than **1** against *P.*  
7  
8 *falciparum* parasites *in vitro* and indeed are amongst the most potent compounds that have been  
9  
10 identified in the series. However these compounds are less metabolically stable than **1** in mouse  
11  
12 liver microsomes, suggesting the likelihood of higher clearance in mice and explaining the  
13  
14 requirement for higher doses to inhibit parasites in the *in vivo* mouse model of malaria.  
15  
16  
17  
18  
19  
20  
21  
22  
23  
24  
25  
26  
27  
28  
29  
30  
31  
32  
33  
34  
35  
36  
37  
38  
39  
40  
41  
42  
43  
44  
45  
46  
47  
48  
49  
50  
51  
52  
53  
54  
55  
56  
57  
58  
59  
60

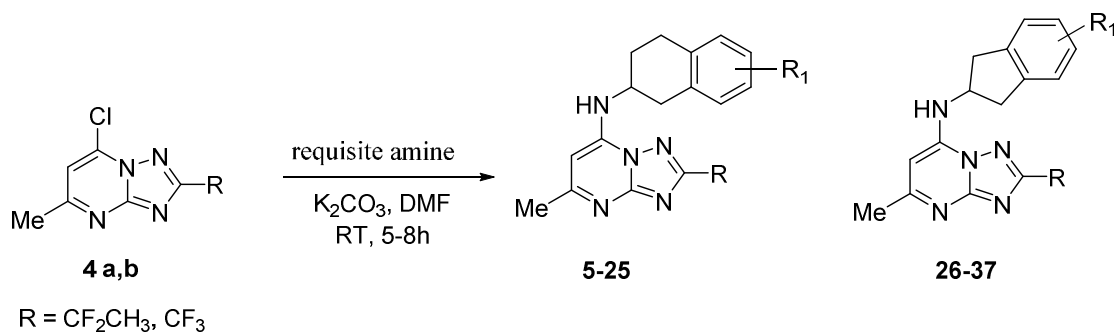
## Chemistry

The focus of the study was to examine the structure activity relationships (SAR) of replacing the p-SF<sub>5</sub>-aniline of **1** with substituted 1,2,3,4-tetrahydro-2-naphthyl or 2-indanyl amines with the goal of eliminating activity on rodent DHODHs, while potentially improving potency against *P. falciparum* DHODH and thereby lowering the dose required for *in vivo* efficacy. The clinical candidate **1** is a potent inhibitor of *Pf*DHODH with only minimal activity detected against human DHODH (selectivity window >5000-fold; Table 1). However, **1** showed inhibitory activity against rodent and to a lesser extent dog DHODHs, although potency towards these enzymes remained considerably less than for *Pf*DHODH.<sup>12</sup> Because these species are required for toxicity testing in preclinical studies we sought to eliminate rodent and dog DHODH inhibitory activity for any potential candidate that might be developed as a backup to **1**. We previously reported that substitution of the p-SF<sub>5</sub>-aniline with p-CF<sub>3</sub> aniline in the context of either mono or difluoro groups at the meta position led to greater inhibition of the mammalian enzymes.<sup>18</sup> X-ray structural data suggested that increasing hydrophobicity drove the interaction of these compounds with the mammalian enzymes. We hypothesized based on these structures that increasing the size of the aromatic amine might prevent binding to mammalian DHODHs, while increasing potency towards the parasite enzyme. We previously tested several tetrahydro-2-naphthyl and 2-indanyl amines as substitutes for the CF<sub>3</sub>-aniline of **3** but found these compounds lacked potency and furthermore, the one analog containing 1,2,3,4-tetrahydro-2-naphthyl also lacked metabolic stability in mouse microsomes.<sup>19</sup> However, these amines were never tested within the context of haloalkyl groups (CF<sub>2</sub>CH<sub>3</sub> or CF<sub>3</sub>) at the C2 position of the triazolopyrimidine ring, which was a key substitution required to boost the potency of the series.<sup>11</sup> We therefore synthesized a series of tetrahydro-2-naphthyl or 2-indanyl analogs with halo alkyl groups at the C2 position. Substituents (halo, haloalkyl, Me, CF<sub>3</sub>, OMe and SO<sub>2</sub>Me

and SO<sub>2</sub>NMe<sub>2</sub>) were incorporated onto the tetrahydro-2-naphthyl or 2-indanyl aromatic rings to improve metabolic stability over the unsubstituted analogs.

The synthetic strategy to generate the appropriately substituted triazolopyrimidines has previously been described.<sup>11, 15, 16</sup> For the studies described herein, 7-chloro-2-(1,1-difluoroethyl)-5-methyl[1,2,4]triazolo[1,5-a] pyrimidine (**4a**) and 7-chloro-2-(trifluoromethyl)-5-methyl[1,2,4]triazolo[1,5-a] pyrimidine (**4b**) were prepared using these methods (Scheme 1) and were reacted with the requisite amines to afford the final products containing either the 1,2,3,4-tetrahydro-2-naphthyl (**5-25**) or 2-indanyl (**26-37**) amines in place of the p-SF<sub>5</sub>-aniline of **1**. Most amines utilized for the study were commercially available with the exception that amines for compounds **29-37**, were synthesized as described in Scheme 2 and supplementary Scheme S1. The 1,2,3,4-tetrahydro-2-naphthyls contained a chiral center and for select compounds, individual enantiomers were purified using a chiral column as described in the experimental section.

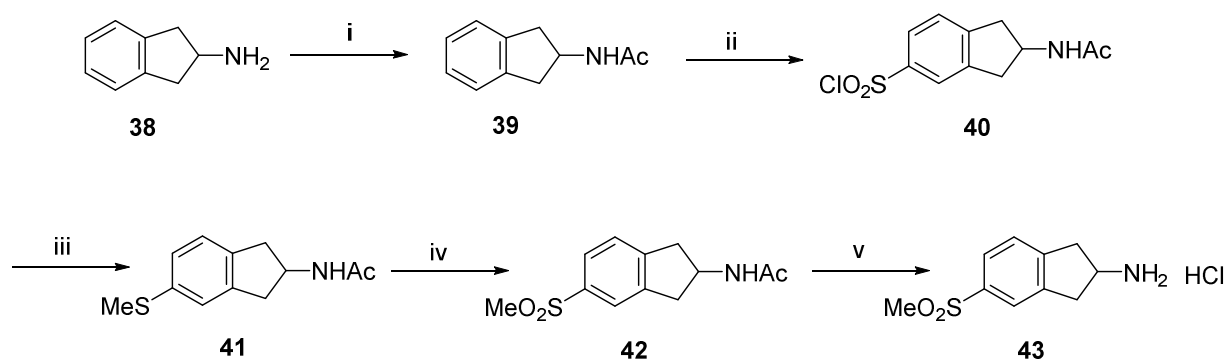
### Scheme 1. General synthetic method



The amine precursor 5-(methylsulfonyl)-2,3-dihydro-1H-inden-2-amine HCl **43** was prepared in five steps (Scheme 2). First, 2-aminoindane **38** was acetylated with acetic anhydride-sodium acetate to yield the acetamido derivative **39**. Further, regioselective chlorosulfonylation

of **39** led to the sulfonylchloride intermediate **40**. Reduction of the sulfonylchloride to the thiol was achieved by tin chloride, which was converted to a methylthio derivative **41** using sodium methoxide, methyl iodide. Next, oxidation of methylthio intermediate **41** with mCPBA gave the acetyl protected methanesulfonyl derivative **42**. Upon deprotection of this acetyl group using 3N HCl, the required amine precursor **43** was obtained.

**Scheme 2. Synthesis of 5-(methylsulfonyl)-2,3-dihydro-1H-inden-2-amine. HCl (43)**



<sup>a</sup>Reagents and conditions: (i) Ac<sub>2</sub>O, NaOAc, AcOH, RT, 12h; (ii) ClSO<sub>3</sub>H, CHCl<sub>3</sub>, RT, 1h; (iii) (a) SnCl<sub>2</sub> · 2H<sub>2</sub>O, AcOH, HCl, RT, 2h; (b) NaOMe, MeI, MeOH; (iv) mCPBA, CHCl<sub>3</sub>; (v) 3N HCl.

## Results

### *Optimization of inhibitor potency and selectivity.*

Compounds were first analyzed for potency against *P. falciparum*, *P. vivax* and human DHODH, and for activity on *P. falciparum* parasites *in vitro* (Table 1). Compounds in the series showed IC<sub>50</sub>'s against *Pf*DHODH in the range of 0.005 – 8 μM, and EC<sub>50</sub>'s against *P. falciparum* 3D7 parasites in whole cell assays between 0.00039 – 6.5 μM (Table 1). Generally, the tetrahydro-2-naphthyl compounds (**5-25**) were more potent in both assays than the 2-indanyls (**26-37**). The most potent analogs based on the whole cell *P. falciparum* assay were **9** and **13**, both of which contain a halogen (chloro or bromo, respectively) in the 7 position. Compound **13** is the most potent analog identified in the triazolopyrimidine series that has been reported. Overall the trend was for 7 substituted tetrahydro-2-naphthyls to be more potent than those with substitutions at the 6 position. Compounds with Br and Cl substituents (**7, 9, 11, 13**) were more potent than those with fluoro **6**, OMe (**15, 16**) or with disubstitutions (**19, 20, 21**), with the least active tetrahydro-2-naphthyl **21** containing a 6-CF<sub>3</sub>, 7-F. Potency of **21** in the whole cell parasite assay was worse than expected based on the inhibitory activity against *Pf*DHODH, suggesting that the compound may be poorly transported into the parasite. Analogs with CF<sub>3</sub> at C2 (**22, 23, 24**) on the triazolopyrimidine ring were less active than those with CF<sub>2</sub>CH<sub>3</sub> (**5, 6, 9**) at this position. Within the indanyl series the most potent compounds were **32** and **36** containing 4,7 dimethyl or 4-CF<sub>3</sub> substituents respectively, while the least active compounds were **30** and **31** containing 5-SO<sub>2</sub>Me or 5-SO<sub>2</sub>NMe<sub>2</sub> substituents, respectively.

For the tetrahydro-2-naphthyls where individual enantiomers were characterized, differences in potency between the active enantiomer (**7, 9, 11, 13, 16, 19, 24**) and the inactive

1  
2  
3 enantiomer (**8**, **10**, **12**, **14**, **17**, **18**, **25**) ranged from 20-360-fold towards *Pf*DHODH and from 30-  
4  
5 2000-fold against *P. falciparum* 3D7 parasites. The small molecule X-ray structure of the active  
6  
7 enantiomer **9** was solved demonstrating that it was in the *S* configuration (Fig. S1 and Table S1).  
8  
9 We did not isolate the individual enantiomers for compounds from the indane series (**27**, **28**, **30**,  
10  
11 **31**, **34** and **36**), and it is likely that the purified active enantiomers would also show higher  
12  
13 activity for these compounds as well. Thus the reported potency data for the racemic mixture  
14  
15 likely overestimates the true IC<sub>50</sub> by ~2-fold.  
16  
17  
18  
19

20  
21 Overall we observed a good correlation between potency on *Pf*DHODH and potency on  
22  
23 3D7 *P. falciparum* parasites (Fig. S2). There was a tendency for the most potent compounds on  
24  
25 the parasite to show lower potency against *Pf*DHODH, but this difference is likely caused by the  
26  
27 complication of stoichiometric binding for compounds with IC<sub>50</sub>'s at or below the concentration  
28  
29 of enzyme used in the assay (*Pf*DHODH = 5 nM). In order to confirm that for the most potent  
30  
31 compounds parasite killing is due to DHODH inhibition, we tested select compounds (**9** and **13**)  
32  
33 for their ability to inhibit growth of a genetically engineered parasite strain that expresses yeast  
34  
35 DHODH (D10 yDHODH<sup>20</sup>). This strain is resistant to DHODH inhibitors if their mechanism of  
36  
37 action is on target. The EC<sub>50</sub>'s (D10 yDHODH EC<sub>50</sub> = 8.6 and 7.4 μM for **9** and **13**, respectively)  
38  
39 for both compounds were increased by >600-fold against this parasite strain relative to the wild-  
40  
41 type 3D7 parasites, supporting DHODH inhibition as their mechanism of action (Table 1 and  
42  
43 Fig. S3). The addition of proguanil did not reverse the resistance of this strain, which is also  
44  
45 consistent with DHODH as the mechanism of parasite killing. In contrast, it has been previously  
46  
47 reported that proguanil reverses the atovaquone resistance phenotype of the D10 yDHODH  
48  
49 parasite strain, providing a mechanism to distinguish between DHODH and bc1 targeted parasite  
50  
51 growth inhibition.<sup>20</sup> The weak but detectable activity observed on the D10 yDHODH parasites  
52  
53  
54  
55  
56  
57  
58  
59  
60

1  
2  
3 for both compounds suggests that at high concentrations there is a secondary target. For a couple  
4  
5 of select compounds (**9** and **35**) whole cell activity was also tested on several additional cell lines  
6  
7 including chloroquine and pyrimethamine resistant parasites (Table S2). Both compounds were  
8  
9 equally active on all tested strains.  
10  
11

12  
13  
14 Species selectivity was first evaluated by testing against human and *P. vivax* DHODH  
15  
16 (Table 1) and then for a selection of the more potent compounds, inhibitor activity was also  
17  
18 measured for mouse, rat and dog DHODH (Table 2). None of the compounds showed any  
19  
20 inhibition of human DHODH up to the highest tested concentration (100  $\mu$ M), which is similar to  
21  
22 results for **1**. However unlike **1**, none of the compounds showed any activity against either the  
23  
24 rodent or dog DHODHs (Table 2), demonstrating that we had achieved our objective of  
25  
26 eliminating mammalian DHODH activity. Measured IC<sub>50</sub>'s for *P. vivax* DHODH ranged from  
27  
28 1.5 – 10-fold higher than for *Pf*DHODH. The 7-position substituted tetrahydro-2-naphthyls, **9**  
29  
30 and **13** showed minimal differences (1.5 - 3-fold) between the two enzymes suggesting that they  
31  
32 would show good activity against both *P. falciparum* and *P. vivax* parasites, whereas the 6  
33  
34 position compounds (**7** and **11**) had 5 - 8-fold lower activity on *P. vivax* than *P. falciparum*  
35  
36 DHODH.  
37  
38  
39  
40  
41  
42

#### 43 *X-ray structure of 13 bound to PfDHODH.*

44  
45

46 In order to understand the structural basis for the superior potency of **13** we solved its X-ray  
47  
48 structure bound to *Pf*DHODH. The structure was solved to 2.32 Å resolution at an R<sub>work</sub> and R<sub>free</sub>  
49  
50 of 0.18 and 0.21, respectively (Fig. 2 and Table S3). Strong electron density was observed for the  
51  
52 entirety of **13** (Fig. S4A). Compound **13** was oriented in the pocket similarly to other  
53  
54 triazolopyrimidines (e.g. **1** - **3**<sup>12, 17, 18</sup>) with the triazolopyrimidine ring bound adjacent to the  
55  
56  
57  
58  
59  
60

1  
2  
3 flavin cofactor in position to form H-bond interactions with Arg-265 and His-185 (Fig. 2 and  
4 S4B). The tetrahydro-2-naphthyl moiety bound in a hydrophobic pocket forming edge-to-face  
5 stacking interactions with Phe-227 and Phe-188 and was in a very similar orientation to what we  
6 previously observed for the naphthyl moiety of **2** (Fig. 2). Some modest conformational  
7 differences in ring geometry were observed reflecting the difference between the fully planer and  
8 aromatic naphthyl and the puckered configuration of the non-aromatic ring of the tetrahydro-2-  
9 naphthyl. A halogen bond was observed between the 7-bromo group on the tetrahydro-2-  
10 naphthyl of **13** and Cys-233 SH, which likely provides significant binding energy to the enzyme  
11 inhibitor interaction. This is a novel interaction that has not been previously observed.  
12  
13  
14  
15  
16  
17  
18  
19  
20  
21  
22  
23

#### 24 *Physicochemical properties and plasma protein binding*

25  
26  
27  
28 Selected compounds were evaluated for their physicochemical properties to determine if  
29 they had good drug-like properties. Analysis included *in silico* calculations, chromatographic  
30 estimation of Log D (pH 7.4), aqueous solubility and plasma protein binding (Tables 3 and 4).  
31 Tested compounds had physicochemical properties that are suggestive of good oral absorption  
32 (MW <430, H bond donors  $\leq 2$ , H bond acceptors  $\leq 6$ , polar surface area <70 Å<sup>2</sup>). Log D ranged  
33 from 3.1 – 4.1 and the more potent analogs tended to have higher Log D values. Aqueous  
34 solubility (pH 6.5) was poor (1.6 – 6.3 µg/mL) to moderate (12.5 – 25 µg/mL), and in general  
35 compounds in this series had lower kinetic solubility than **1** (Table 3). More extensive solubility  
36 studies in simulated gastric and intestinal fluids was conducted on a selection of the most potent  
37 analogs from the 2-indanyl (**35**) and the tetrahydro-2-naphthyl (**7**, **9**, **11**, **13**) series (Table 4). All  
38 five compounds had better solubility than **1** in 0.1 N HCl. Solubility in fasted-state simulated  
39 intestinal fluid was similar to or slightly improved compared to **1**. The tetrahydro-2-naphthyl  
40  
41  
42  
43  
44  
45  
46  
47  
48  
49  
50  
51  
52  
53  
54  
55  
56  
57  
58  
59  
60

1  
2  
3 compounds substituted at the 6 position (**11** and **7**) showed considerably better solubility in fed-  
4  
5 state simulated intestinal fluid than either **1** or the 7 position (**9** and **13**) substituted compounds.  
6  
7

8  
9 Human, rat and mouse plasma protein binding (PPB) was assessed for the more potent  
10  
11 compounds that were progressed to *in vivo* pharmacokinetic testing (**7**, **9**, **11**, **13**, **35**). The  
12  
13 tetrahydro-2-naphthyl compounds substituted at the 6 position (**7** and **11**) showed higher protein  
14  
15 binding compared to the compounds substituted at the 7 position (**9** and **13**). Binding was similar  
16  
17 across the species tested for each of the compounds. By comparison, **1** exhibited high protein  
18  
19 binding in human and mouse plasma but lower binding in rat plasma. The indanyl analog **35** had  
20  
21 considerably lower protein binding compared to either **1** or the tetrahydro-2-naphthyl  
22  
23 compounds.  
24  
25  
26

#### 27 28 *In vitro* metabolism.

29  
30  
31 To obtain a preliminary indication of the likelihood that compounds would show good *in*  
32  
33 *vivo* pharmacokinetic properties, selected compounds were analyzed for metabolic stability *in*  
34  
35 *vitro* using human, rat and mouse liver microsomes. We previously found that the *in vitro*  
36  
37 microsomal stability of compounds from the triazolopyrimidine series provided a good rank  
38  
39 order estimation of which compounds would have the highest *in vivo* exposure.<sup>11, 15, 16, 19</sup> We  
40  
41 report in Table 3 the *in vitro* intrinsic clearance ( $CL_{int}$ ,  $\mu\text{L}/\text{min}/\text{mg}$  microsomal protein) and the  
42  
43 predicted *in vivo* intrinsic clearance ( $\text{mL}/\text{min}/\text{kg}$ ) obtained using physiologically-based scaling  
44  
45 factors as previously described.<sup>21</sup> Given the early stage of optimization for the series, protein  
46  
47 binding was not determined for all compounds and therefore no attempt was made to predict the  
48  
49 *in vivo* blood clearance (which requires corrections for both plasma and microsomal binding). *In*  
50  
51 *vitro*  $CL_{int}$  values of  $<20 \mu\text{L}/\text{min}/\text{mg}$  protein were taken as being suggestive of good metabolic  
52  
53  
54  
55  
56  
57  
58  
59  
60

1  
2  
3 stability, assuming that clearance only occurs via hepatic metabolism. Overall, the substituted  
4 tetrahydro-2-naphthyls showed good metabolic stability in human liver microsomes but they  
5 were less stable in mouse microsomes (Table 3). Chloro, bromo and CF<sub>3</sub> substituted compounds  
6 (7, 9, 11, 12, 13, 20, 21) were marginally more metabolically stable than the fluoro (6, 19) or  
7 OMe 16 substituted compounds.  
8  
9

10  
11  
12  
13  
14  
15  
16 With the exception of 35, the indanyl analogs were generally metabolically unstable  
17 showing high intrinsic clearance in mouse liver microsomes and moderate to high values in  
18 human and rat microsomes. The least stable compounds were the unsubstituted 2-indanyl 26 and  
19 the 4,7 dimethyl substituted derivative 32. Replacement of both methyl groups with fluorines 33  
20 did not improve stability, although perhaps surprisingly the single 4-F derivative 34 was  
21 significantly more stable. Substantial improvement in metabolic stability was obtained by  
22 moving the fluorines to the 5 and 6 positions of the ring 35, leading to low intrinsic clearance in  
23 human and rat microsomes and moderate clearance in mouse microsomes. These data suggested  
24 that 35 would show good plasma exposure in both mice and rats.  
25  
26  
27  
28  
29  
30  
31  
32  
33  
34  
35  
36  
37

### 38 *hERG channel activity and CYP inhibition.*

39  
40

41 In order to evaluate any potential cardiac risks, select compounds were tested for  
42 inhibition of the human ether-a-go-go-related gene (hERG) K<sup>+</sup> channel in a standard patch clamp  
43 assay. hERG channel inhibition has been associated with QT prolongation and arrhythmias and  
44 patch clamp assays have become a routine method to provide an initial analysis that a compound  
45 may potentially be associated with QT syndromes in humans.<sup>22</sup> Compounds in both the  
46 tetrahydro-2-naphthyl and 2-indanyl series inhibited the hERG channel with IC<sub>50</sub>'s in the range  
47 of 0.5 – 1.8 μM (Table 3).  
48  
49  
50  
51  
52  
53  
54  
55  
56  
57  
58  
59  
60

1  
2  
3 In order to test for the potential for drug-drug interactions, select compounds were tested  
4  
5 for their ability to inhibit cytochrome P450 isoforms in human liver microsomes (Table 5). All  
6  
7 tested compounds showed moderate inhibition of isoforms 2C9 and 2D6. The most significant  
8  
9 inhibition was observed for **9** and **13** as both inhibited these two isoforms in the 2 – 4  $\mu\text{M}$  range.  
10  
11

12  
13  
14 *In vivo* pharmacokinetic studies in rats and mice.  
15

16  
17 Five of the most potent compounds were selected for assessment of their *in vivo*  
18  
19 pharmacokinetic properties based on their good *in vitro* metabolic stability. Mice were dosed  
20  
21 orally while rats were dosed orally and intravenously to allow determination of the clearance,  
22  
23 volume of distribution and oral bioavailability. Compounds included one from the indanyl series  
24  
25 (**35**) and four from the tetrahydro-2-naphthyl series (**7**, **9**, **11**, **13**).  
26  
27

28  
29 All five compounds showed good exposure over 24 h in both mice and rats after oral  
30  
31 administration (Tables 6 and 7, Figs. 3 and 4). Compounds were well tolerated at the  
32  
33 administered doses and no adverse reactions were observed. In mice,  $C_{\text{max}}$  and  $\text{AUC}_{24\text{h}}$  values  
34  
35 were highest for **35**, and lower for the tetrahydro-2-naphthyl compounds. Compared to **1** and  
36  
37 taking into account the differences in dose, total  $C_{\text{max}}$  and  $\text{AUC}_{24\text{h}}$  values were similar or lower  
38  
39 for the tetrahydro-2-naphthyl compounds, whereas unbound  $C_{\text{max}}$  and  $\text{AUC}_{24\text{h}}$  were similar (for  
40  
41 **7**) or somewhat higher (3-4-fold for **9**, **11**, and **13**). The indanyl (**35**) had the highest plasma  
42  
43 exposure in mice in terms of both total and unbound  $C_{\text{max}}$  and  $\text{AUC}_{24\text{h}}$  and significantly higher  
44  
45 exposure compared to **1**. Similar to **1**, the terminal elimination half-life ( $t_{1/2}$ ) in mice was  $\sim 2$  h for  
46  
47 all five compounds (Table 6 and Fig. 3).  
48  
49  
50  
51  
52

53  
54 In rats, the oral bioavailability was high for all compounds tested, ranging from 63 –  
55  
56 100% compared to 57% for **1** (Table 7 and Fig. 4). The plasma clearance and volume of  
57  
58  
59  
60

1  
2  
3 distribution were significantly lower for the tetrahydro-2-naphthyl compounds substituted on the  
4  
5 6 position (**7** and **11**) than for those substituted on the 7 position (**9** and **13**), however when  
6  
7 corrected for differences in plasma protein binding, values across the four tetrahydro-naphthyl  
8  
9 compounds were comparable (within 2-fold). The 6 position compounds also had lower blood to  
10  
11 plasma partitioning consistent with their higher plasma protein binding compared to the 7  
12  
13 position analogs. Unbound clearance values for the tetrahydro-2-naphthyl compounds were  
14  
15 somewhat lower for the two chloro substituted compounds (438 and 589 mL/min/kg for **7** and **9**,  
16  
17 respectively) compared to the bromo compounds (933 and 800 mL/min/kg for **11** and **13**,  
18  
19 respectively) and all were higher than for **1** (263 mL/min/kg). As a result, unbound AUC values  
20  
21 for the tetrahydro-2-naphthyls were approximately 2-4 fold lower than **1** after oral dosing at  
22  
23 approximately 20 mg/kg. The  $t_{1/2}$  for the tetrahydro-2-naphthyl compounds ranged from 6-7 h in  
24  
25 comparison to 13 h for **1**. The indanyl compound (**35**) had low unbound clearance and volume of  
26  
27 distribution and overall unbound oral exposure was superior to **1** and to the tetrahydro-2-  
28  
29 naphthyls (Table 7).

### 30 31 32 *In vivo efficacy in the SCID mouse model of P. falciparum*

33  
34  
35  
36  
37  
38  
39  
40  
41 Based on the observation of good oral exposure after dosing in mice, we tested three  
42  
43 compounds in the SCID mouse *P. falciparum* efficacy model, which has become the standard  
44  
45 model for evaluating the efficacy of new antimalarial compounds.<sup>23</sup> The tetrahydro-2-naphthyl  
46  
47 compounds substituted at the 7 position (**9** and **13**) were more potent against *P. falciparum* in the  
48  
49 *in vitro* parasite assay than those substituted on the 6 position (**7** and **11**) and showed fairly  
50  
51 equivalent exposure in mice after oral dosing. We therefore decided to test both a 6- and 7-  
52  
53 substituted tetrahydro-2-naphthyl (**7** and **9**) in the *P. falciparum* SCID mouse model. Because **35**  
54  
55 showed significantly higher plasma exposure in mice than the remaining compounds, we also  
56  
57  
58  
59  
60

1  
2  
3 selected this compound for an efficacy study despite the 10-fold lower potency in the *P.*  
4  
5 *falciparum* parasite assay.  
6  
7

8  
9 All three compounds were dosed orally once a day for 4 days and tested for efficacy and  
10 blood concentrations at two doses (10 and 30 mg/kg). Each was well tolerated and there were no  
11 adverse reactions. The effective dose that led to 90% parasite clearance (ED<sub>90</sub>) was calculated  
12 24 h after the last dose (Table 8 and Fig. 5A). Pharmacokinetic sampling was performed on day  
13 1 to allow the total blood AUC at the ED<sub>90</sub> to be assessed (Tables 8 and S4 and Fig. 5B).  
14 Because of the complicated nature of blood in the SCID mouse model (i.e. mice contain a  
15 mixture of human and mouse plasma and erythrocytes and a hematocrit of 70-80%), it was not  
16 possible to accurately convert blood concentrations to plasma concentrations or to correct  
17 concentrations for differences in plasma protein binding.  
18  
19  
20  
21  
22  
23  
24  
25  
26  
27  
28  
29  
30

31 All three compounds showed efficacy in this model, however **9** significantly  
32 outperformed the other two compounds based on ED<sub>90</sub> (Tables 8 and S4 and Fig. 5). The ED<sub>90</sub>  
33 was higher for all three compounds than for **1** ranging from ~19 mg/kg for **9** to > 30 mg/kg for **7**  
34 and **35**. The pharmacokinetic data indicated that as expected, **35** exhibited higher total blood  
35 concentrations than the other two compounds. Both **7** and **9** were approximately dose linear for  
36 both C<sub>max</sub> and AUC, whereas **35** showed significant non-linearity and evidence of a second peak  
37 at 8 h at the lower dose (Table S4). Despite requiring a higher dose, **9** showed higher apparent  
38 efficacy compared to **1** based on the total blood AUC at the ED<sub>90</sub> which was 5-fold lower than  
39 that required for **1** in the once daily dosing regimen (Table 8). However, when accounting for  
40 differences in the plasma unbound fractions for **1** and **9** (approximately 0.002 for **1** and 0.03 for  
41 **9**, Table 3), **1** likely has lower unbound concentrations at the ED<sub>90</sub>, and hence higher intrinsic  
42 efficacy. In contrast, **35** was significantly less effective than **1** suggesting that the lower intrinsic  
43  
44  
45  
46  
47  
48  
49  
50  
51  
52  
53  
54  
55  
56  
57  
58  
59  
60

1  
2  
3 potency of **35** could not be overcome by higher exposure levels. The  
4  
5 pharmacokinetic/pharmacodynamic relationship for **7** could not be evaluated in detail as the  
6  
7  
8 ED<sub>90</sub> was not reached in this study.  
9  
10  
11  
12  
13  
14  
15  
16  
17  
18  
19  
20  
21  
22  
23  
24  
25  
26  
27  
28  
29  
30  
31  
32  
33  
34  
35  
36  
37  
38  
39  
40  
41  
42  
43  
44  
45  
46  
47  
48  
49  
50  
51  
52  
53  
54  
55  
56  
57  
58  
59  
60

## Discussion

Malaria is one of the most serious global infectious diseases and while a number of effective drugs have been used to treat malaria, drug resistance has led to the loss of most agents that have been in wide spread use.<sup>2</sup> A robust drug pipeline is therefore key to malaria control and elimination efforts.<sup>4</sup> DHODH has emerged as a key new target in efforts to identify antimalarial drugs that work on clinical isolates resistant to standard therapies and as noted, the triazolopyrimidine **1**, is currently in clinical development.<sup>12</sup> In order to identify potential backup compounds to **1** in case issues arise in its clinical development, we sought to identify additional compounds within the triazolopyrimidine series with the potential to advance into preclinical development. One identified potential liability of **1** has been the finding that while it does not inhibit human DHODH, it does show moderate inhibition of the mouse and rat enzymes, which complicates toxicity testing in animals. We therefore sought to identify new derivatives that showed broad selectivity against all of the key mammalian enzymes. Herein we describe a series of tetrahydro-2-naphthyl and 2-indanyl triazolopyrimidine analogs, which display a range of potencies against *Plasmodium* DHODH, but which importantly lack activity against human DHODH or any of the key mammalian enzymes from species that are important for toxicological profiling (mouse, rat and dog). Pharmacologic profiling and *in vivo* efficacy assays suggest that several of the identified analogs have potential, with **9** showing the most promising profile.

In evaluating the tetrahydro-2-naphthyl and 2-indanyl triazolopyrimidine analogs we found that the tetrahydro-2-naphthyls (e.g. **7**, **9**, **11**, **13**) had significantly greater potency on *Pf*DHODH and *Plasmodium* parasites in whole cell assays than the 2-indanyl analogs (e.g. **35**). The most potent of the tetrahydro-2-naphthyl derivatives also showed good activity (within 1.5-fold) against *P. vivax* DHODH suggesting that they would be useful for the treatment of both *P.*

1  
2  
3 *falciparum* and *P. vivax*. In contrast, the best of the 2-indanyl analogs (**35**) was 7-fold less active  
4  
5 on *P. vivax* DHODH suggesting it might not have good activity against the *P. vivax* parasite.  
6  
7

8  
9 The X-ray structure of the 7-bromo analog **13** showed that in addition to the previously  
10  
11 observed H-bonds and stacking interactions observed for other analogs in the series,<sup>11, 12, 17, 18</sup> a  
12  
13 good halogen bond was formed between the bromo group of **13** and Cys-233 that is likely to  
14  
15 provide considerable binding energy to the interaction. Indeed halogen bonding to protein  
16  
17 residues that include Lewis bases (e.g. sulfur) are commonly observed in protein structures  
18  
19 deposited in the PDB.<sup>24</sup> The overall binding mode of **13** is very similar to that of **2**, which was  
20  
21 expected based on their close structural similarity. Like the naphthyl of **2**, the tetrahydro-2-  
22  
23 naphthyl of **13** better fills the available binding pocket than the SF<sub>5</sub>-aniline of **1**, which supports  
24  
25 our initial hypothesis that compounds with improved potency could be identified by substitution  
26  
27 of the SF<sub>5</sub>-aniline with bulkier aromatic groups.  
28  
29  
30  
31  
32

33 Comparison of the tetrahydro-2-naphthyl compounds containing 7 position (**9** and **13**)  
34  
35 versus 6 position (**7** and **11**) substitutions identified a number of interesting differences. Analogs  
36  
37 substituted in the 7 position were more potent than 6 position analogs, and indeed **13** with sub  
38  
39 nanomolar activity against the parasite in whole cell assays is the most potent analog that has  
40  
41 been identified in the series. However these assays did not take into account potential differences  
42  
43 in protein binding. The 6 position analogs exhibited consistently higher plasma protein binding  
44  
45 than the 7 position compounds and a similar trend is also likely for binding to albumax present in  
46  
47 the *in vitro* test medium. Assessment of the pharmacologic properties showed that while the 7  
48  
49 position tetrahydro-2-naphthyls had greater apparent antimalarial potency, analogs substituted at  
50  
51 the 6 position had somewhat improved physicochemical properties. The 6 position analogs **7** and  
52  
53 **11** were more soluble (in 0.1 N HCl and FeSSIF media) than either of the 7 position analogs (**9**  
54  
55  
56  
57  
58  
59  
60

1  
2  
3 and **13**). While the total plasma exposure (AUC and  $C_{max}$ ) in rats was higher for the 6 position  
4  
5 analogs, correction of the data for protein binding indicated that the unbound exposure and  
6  
7 unbound clearance were similar (within 2-fold) for the 6 and 7 position analogs with the chloro  
8  
9 substituted compounds (**7** and **9**) showing about 2-fold lower unbound clearance than the bromo  
10  
11 substituted compounds (**11** and **13**). So while total exposure appears greater for the 6 position  
12  
13 analogs, unbound concentrations are comparable across the tetrahydro-naphthyl compounds  
14  
15 tested. Protein binding data in mouse plasma was only available for **9**, **11** and **35** and binding for  
16  
17 each of these compounds was similar in each of the three species tested. Mouse plasma protein  
18  
19 binding was therefore estimated for **7** and **13** using the average of the human and rat values,  
20  
21 suggesting that unbound concentrations for each of the compounds are likely to be within a  
22  
23 similar range (Table 6). The best of the 2-indanyl analogs (**35**) had considerably higher unbound  
24  
25 plasma exposure in rats compared to the tetrahydro-2-naphthyls and to **1**, and had similarly low  
26  
27 unbound clearance.  
28  
29  
30  
31  
32

33  
34  
35 The *in vitro* data generated in liver microsomes provided a mechanism to rank  
36  
37 compounds based on their relative metabolic stability. The compounds selected for *in vivo*  
38  
39 testing were expected to have good exposure, and this was seen following dosing to both rats and  
40  
41 mice indicating that qualitatively, the *in vitro* data were informative. Converting the *in vitro*  
42  
43 intrinsic clearance determined in rat microsomes to a plasma clearance using physiologically-  
44  
45 based scaling factors and taking into account binding to rat plasma and microsomal proteins (as  
46  
47 per <sup>21</sup>) and blood to plasma partitioning ratio led to an under prediction of the actual *in vivo*  
48  
49 clearance by a factor of 3- to 16-fold for the five compounds tested. These trends are similar to  
50  
51 what had been observed previously for **1**<sup>16</sup> and suggest that *in vivo* clearance mechanisms for the  
52  
53 series also involve additional non-CYP pathways not fully represented by the microsomal test  
54  
55  
56  
57  
58  
59  
60

1  
2  
3 system. In the case of **1**, hepatocyte assays also led to an under prediction of *in vivo* clearance  
4 highlighting the difficulties in obtaining accurate clearance predictions based on *in vitro* data  
5  
6 alone. Further studies with the current compounds using hepatocytes may have provided  
7  
8 additional insight into their clearance mechanisms.  
9  
10

11  
12  
13 *In vivo* efficacy was assessed in the *P. falciparum* SCID mouse model. Of the three tested  
14 compounds, **9** (7 position) had the most potent *in vivo* activity. The total blood AUC required to  
15 reach ED<sub>90</sub> was lower than for **1**, however it took a higher dose (~19 mg/kg versus 8.1 mg/kg for  
16 QD dosing) to achieve this activity, possibly due to a higher unbound clearance of **9** compared to  
17  
18 **1** as seen in rats. The binding trends in human and mouse plasma would suggest that unbound  
19 concentrations of **9** in the SCID mouse are likely to be considerably higher compared to those for  
20  
21 **1** at the same total blood concentration. Therefore, the true *in vivo* potency of **1** based on  
22 unbound concentrations is likely to be greater than that for **9**. In spite of the high blood exposure,  
23 the 2-indanyl (**35**) lacked sufficient intrinsic potency to provide good activity in the *in vivo*  
24 model. In order to improve patient compliance, single dose treatments are being sought by the  
25 international organizations that are promoting new drug discovery for malaria.<sup>4</sup> While all three  
26 tested compounds (**7**, **9** and **35**) showed *in vivo* antimalarial activity, it is unlikely that any of  
27 these compounds have the necessary properties to support a single dose treatment regimen at a  
28 practical dose level in humans.  
29  
30  
31  
32  
33  
34  
35  
36  
37  
38  
39  
40  
41  
42  
43  
44  
45  
46

47 Preliminary safety analysis included characterizing hERG channel activity to assess  
48 potential cardiac effects and CYP inhibition studies to determine the potential for drug-drug  
49 interactions. All five of the profiled compounds showed some CYP inhibition, with CYP isoform  
50 2D6 being inhibited to the greatest extent. CYP2D6 inhibition was modest with the most potent  
51 inhibition observed in the 3 – 6  $\mu$ M range, but does suggest some potential for drug-drug  
52  
53  
54  
55  
56  
57  
58  
59  
60

1  
2  
3 interactions with compounds that are substrates for this enzyme. Tested compounds in these  
4 series also showed some hERG inhibition (0.5 – 1.5  $\mu\text{M}$  range). This inhibitory activity is similar  
5 to what was observed for **1**, where subsequent studies using the rabbit wedge model and dog  
6 cardiovascular studies showed no evidence for QT prolongation, arrhythmias or cardiac effects.<sup>12</sup>  
7  
8 Additionally, for **1** the unbound plasma concentration at likely therapeutic doses is 70-320-fold  
9 lower than the  $\text{IC}_{50}$  for hERG channel inhibition, suggesting it would be very unlikely that **1**  
10 would inhibit the channel *in vivo*. Insufficient efficacy data is available for compounds **7** and **35**  
11 to determine the safety margin relative to unbound concentrations at an efficacious dose,  
12 however for **9** the  $\text{C}_{\text{max}}$  at the  $\text{ED}_{90}$  in the SCID study (unbound concentration of approximately  
13 0.05  $\mu\text{M}$ ) is  $\sim$ 30-fold lower than the  $\text{IC}_{50}$  on the hERG channel, again suggesting a low  
14 likelihood the channel would be inhibited *in vivo*. However given the hERG channel activity,  
15 careful evaluation of cardiac safety would be an important component of preclinical development  
16 if any of these compounds were to be advanced.  
17  
18  
19  
20  
21  
22  
23  
24  
25  
26  
27  
28  
29  
30  
31  
32  
33

34  
35 Several potential avenues remain feasible for additional optimization of the  
36 triazolopyrimidine series. Firstly, only the chloro substituted tetrahydro-2-naphthyls were tested  
37 in the SCID efficacy model, leaving open the possibility that one of the bromo analogs might  
38 have shown better *in vivo* efficacy. Additional optimization of the series might focus on reducing  
39 lipophilicity as this could lead to reduced intrinsic clearance and better *in vivo* exposure and also  
40 could lead to reduced hERG activity. Reduced lipophilicity would also likely result in improved  
41 aqueous solubility thereby simplifying formulation approaches for oral administration.  
42 Decreasing lipophilicity will likely require the  $\text{SF}_5$ -aniline of **1** to be replaced with more  
43 hydrophilic aromatic amines, provided potency can be maintained. Within the tetrahydro-2-  
44  
45  
46  
47  
48  
49  
50  
51  
52  
53  
54  
55  
56  
57  
58  
59  
60

1  
2  
3 naphthyls, it might yet be possible to identify more metabolically stable analogs by identifying  
4  
5 the specific sites of metabolism and attempting to block them.  
6  
7

## 8 9 **Conclusion**

10  
11 We have described the identification of several tetrahydro-2-naphthyl and 2-indanyl  
12  
13 triazolopyrimidine analogs that are potent inhibitors of *Plasmodium* DHODH and which have  
14  
15 improved species selectivity over the mammalian enzymes in comparison to the clinical  
16  
17 candidate **1**. The compounds have potent activity against *P. falciparum* in parasite assays and  
18  
19 showed antimalarial activity in the *P. falciparum* SCID mouse model of disease. These  
20  
21 compounds showed good plasma exposure after oral dosing in mice and rats and were well  
22  
23 tolerated in the *in vivo* studies that were performed. Several of the identified compounds, most  
24  
25 notably **9**, have the potential to be further developed for treatment of malaria. However, the  
26  
27 findings that **9** is less intrinsically potent than **1** *in vivo* (based on expected unbound  
28  
29 concentrations) and that the unbound clearance in rat is 2-fold higher than for **1**, suggest that this  
30  
31 compound is unlikely to meet the strict criteria required for a single dose cure at a reasonable  
32  
33  
34  
35  
36  
37  
38  
39  
40  
41  
42  
43  
44  
45  
46  
47  
48  
49  
50  
51  
52  
53  
54  
55  
56  
57  
58  
59  
60  
dose.

## Experimental section.

### *DHODH purification.*

Plasmodium and mammalian DHODHs were expressed in *E. coli* as N-terminal truncations (lacking the mitochondrial transmembrane domains) fused to His<sub>6</sub>-purification tags as previously described.<sup>11, 17, 18, 25</sup> Protein (*Pf*DHODH $_{\Delta 384-413}$ ) for crystallization studies was further truncated to remove a proteolytically sensitive loop (amino acids 384-421) that prevents crystallization as previously described.<sup>17, 26</sup> Proteins were expressed in *E. coli* BL21 phage-resistant cells (Novagen) and they were purified by Ni<sup>+2</sup>-agarose column chromatography (GE Healthcare Life Sciences, HisTrap HP) and Gel-filtration column chromatography (GE Healthcare Life Sciences, HiLoad 16/600 Superdex 200 pg) as previously described.<sup>11, 17, 18</sup> Protein was concentrated to 10-30 mg/ml and stored at -80°C.

### *DHODH kinetic analysis.*

Steady-state kinetic analysis was performed using a dye-based spectrophotometric method in assay buffer (100 mM HEPES, pH 8.0, 150 mM NaCl, 10% glycerol, 0.05% Triton X-100) as previously described.<sup>11</sup> All buffers were degassed prior to use. Enzyme and substrate concentrations were: DHODH (E = 5 nM), substrates (0.2 mM L-dihydroorotate, 0.02 mM CoQ<sub>d</sub> and 0.12 mM 2,5-dichloroindophenol (DCIP)). Inhibitor stock solutions (100 mM) were made in DMSO and protected from light in dark amber vials. Serial dilutions were then performed to generate a 3-fold dilution series of 100x stocks also in DMSO that were used in the final assay (final inhibitor concentration range was 0.01 – 100  $\mu$ M). Data were collected in triplicate for each concentration in the titration. Data were fitted to the log[I] vs response (three parameters) equation to determine the concentration that gave 50% enzyme inhibition (IC<sub>50</sub>) except for

1  
2  
3 compounds where the  $IC_{50} > 10 \mu M$  which were instead fitted to the standard  $IC_{50}$  equation  
4  
5  $(Y=1/(1+X/(IC_{50})))$  in Graphpad Prism. Error represents the 95% confidence interval of the fit.  
6  
7

8 *P. falciparum* growth assays.

9  
10  
11 *P. falciparum* parasites were grown in RPMI-1640 containing 0.5% Albumax-II as  
12  
13 previously described.<sup>11</sup> Inhibitor stock solutions were prepared as described above for DHODH  
14  
15 kinetic analysis except that a 500x dilution series prepared in DMSO was used to generate a 10x  
16  
17 dilution series in RPMI so that final DMSO concentration in the media was 0.2%. Growth  
18  
19 assays for *P. falciparum* 3D7 cells and drug-resistant parasites were performed using the SYBR-  
20  
21 green 72 h growth assay.<sup>18</sup> Data were collected in triplicate to quadruplicate for each  
22  
23 concentration in the titration. Data were fitted to the log[I] vs response Variable slope (four  
24  
25 parameter) equation in graph pad prism to determine the effective concentration ( $EC_{50}$ ) that led  
26  
27 to 50% reduction in parasitemia. Error represents the 95% confidence interval of the fit.  
28  
29  
30  
31  
32

33 *In vitro* metabolism and physicochemical assessment.

34  
35  
36  
37 *In vitro* metabolism. Selected compounds were incubated at a concentration of 1  $\mu M$  with  
38  
39 mouse, rat or pooled human liver microsomes (BD Gentest, Woburn, MA or XenoTech LLC,  
40  
41 Lenexa, Kansas City) at a microsomal protein concentration of 0.4 mg/mL.<sup>11</sup> Substrate depletion  
42  
43 was assessed by LC-MS. Measured *in vitro* intrinsic clearance values ( $\mu L/min/mg$  microsomal  
44  
45 protein) were converted to predicted *in vivo* intrinsic clearances (mL/min/kg) using published  
46  
47 physiologically based scaling factors.<sup>21</sup>  
48  
49  
50

51  
52 *Solubility.* Aqueous solubility of compounds was assessed by nephelometry as described  
53  
54 previously.<sup>27</sup> Compound stock solutions were prepared in DMSO, which was then spiked into  
55  
56 pH 6.5 phosphate buffer giving a final DMSO concentration of 1%. Solubility measurements in  
57  
58  
59  
60

1  
2  
3 physiologically-relevant media were conducted for selected compounds. Media included 0.1 N  
4 HCl to represent a simulated gastric condition, fasted (FaSSIF, pH 6.5) and fed (FeSSIF, pH 5.0  
5 or 5.8) state simulated intestinal fluids prepared as described previously.<sup>28</sup> Solid material was  
6 incubated in media for a period of 5-6 h at 37°C with periodic mixing and sample supernatant  
7 concentrations determined by HPLC with UV detection following two separate centrifugations to  
8 remove undissolved compound.  
9

### 10 11 12 13 14 15 16 17 18 *Plasma protein binding and partitioning.* 19

20  
21 Select compounds were analyzed for plasma protein binding (PPB) in human, rat, or  
22 mouse plasma using an ultracentrifugation method at 37°C as previously described<sup>11</sup> followed by  
23 LC-MS analysis as described below. Protein binding was calculated by comparing the unbound  
24 concentration in the ultracentrifuged samples to the total plasma concentration in control samples  
25 incubated at 37°C for the same time period. For compounds progressing to rat pharmacokinetic  
26 studies, blood to plasma partitioning ratios in rat blood were also assessed as described  
27 previously<sup>16</sup>.  
28  
29  
30  
31  
32  
33  
34  
35  
36  
37  
38

### 39 *Pharmacokinetic analysis in mice and rats* 40 41

42 Pharmacokinetic studies for select compounds were performed in mice and rats in  
43 accordance with the Australian Code of Practice for the Care and Use of Animals for Scientific  
44 Purposes and the study protocols were approved by the Monash Institute of Pharmaceutical  
45 Sciences Animal Ethics Committee.  
46  
47  
48  
49  
50

51  
52 Oral doses were administered as a suspension in a vehicle containing 0.5% w/v  
53 carboxymethylcellulose, 0.5% v/v benzyl alcohol (as a preservative) and 0.4% v/v Tween 80 and  
54 intravenous doses were administered in co-solvent vehicle containing 40% propylene glycol,  
55  
56  
57  
58  
59  
60

1  
2  
3 10% ethanol, 0.4% Tween 80 in water. IV doses to rats were administered as a 10 min constant  
4  
5 rate infusion of 1 mL into an indwelling jugular vein cannula, and oral doses were administered  
6  
7 by gavage as 10 mL/kg (both rats and mice). Blood was collected from rats via a cannula  
8  
9 inserted into the carotid artery on the day prior to dosing, and from mice via either  
10  
11 submandibular bleed or terminal cardiac puncture (maximum of two samples per mouse) into  
12  
13 tubes containing heparin as an anticoagulant and plasma was separated by centrifugation.  
14  
15 Compound concentrations were quantitated by LC-MS using a Waters Xevo TQ mass  
16  
17 spectrometer coupled to a Waters Acquity UPLC. Chromatography was conducted using a  
18  
19 Supelco Ascentis Express RP Amide column (50 x 2.1mm, 2.7  $\mu$ m) with a mobile phase  
20  
21 consisting of 0.05% formic acid in water and 0.05% formic acid in methanol mixed via a linear  
22  
23 gradient with a cycle time of 4 min. The flow rate was 0.4 mL/min and the injection volume was  
24  
25 3  $\mu$ L. Detection was via positive electrospray ionisation mass spectrometry with multiple-  
26  
27 reaction monitoring using a cone voltage of 30-40 V and collision energy of 25-35 V. Calibration  
28  
29 curves were prepared using blank rat or mouse plasma and validation studies confirmed the  
30  
31 accuracy, precision and limit of quantitation to be within acceptable ranges.  
32  
33  
34  
35  
36  
37  
38

### 39 *Cyp inhibition assays*

40  
41  
42  
43 Inhibition of cytochrome P450 (CYP) enzymes was assessed in human liver microsomes  
44  
45 using a substrate specific approach where the formation of metabolites specific to a particular  
46  
47 CYP isoform was monitored. Microsomes were suspended in phosphate buffer and incubated at  
48  
49 37°C in the presence of probe substrates<sup>29</sup> and reactions were initiated by the addition of an  
50  
51 NADPH-regenerating system. Reactions were quenched at appropriate times using acetonitrile.  
52  
53  
54 Samples were centrifuged and concentrations of the metabolites assessed by LC-MS. The IC50  
55  
56 value for each compound or control inhibitor was the concentration at which there was a 50%  
57  
58  
59  
60

1  
2  
3 reduction in the amount metabolite formed relative to the maximum metabolite formation in the  
4  
5 absence of inhibitor.  
6  
7

8  
9 *hERG analysis.*

10  
11  
12 Select compounds were tested for activity against the human ether-a-go-go related gene  
13 (hERG) K<sup>+</sup> channel in a IonWorks patch clamp electrophysiology assay under contract to Essen  
14  
15 BioScience (Welwyn Garden City Hertfordshire, UK).  
16  
17

18  
19  
20 *SCID mouse efficacy studies.*

21  
22  
23 NOD-*scid IL-2R $\gamma$ mull* (NSG) mice (Jackson Laboratory, USA) (23-36 g) were engrafted  
24 with human erythrocytes and then infected with *P. falciparum* Pf3D7<sub>0087/N9</sub> parasites (20 x 10<sup>6</sup>)  
25  
26 by intravenous injection as described.<sup>23</sup> Compounds (**7**, **9** and **35**) were administered by oral  
27  
28 gavage once daily (QD) for four consecutive days starting on day 3 post infection in vehicle  
29  
30 (0.5% w/v sodium carboxymethylcellulose, 0.5% v/v benzyl alcohol, 0.4% v/v Tween 80 in  
31  
32 water). Parasitemia was monitored by flow cytometry. To verify the actual doses administered  
33  
34 formulation concentrations were measured. Compound levels in the formulations or in the blood  
35  
36 of infected mice were measured by LC/MS/MS as described above. Human biological samples  
37  
38 were sourced ethically and their research use was in accordance with the terms of the informed  
39  
40 consents.  
41  
42  
43  
44  
45

46  
47 *Small molecule X-ray structure determination and refinement of 9.*

48  
49  
50 Compound **9** was crystallized from ethanol. A colorless prism, measuring 0.20 x 0.13 x  
51  
52 0.10 mm<sup>3</sup> was mounted on a loop with oil. Data was collected at -173°C on a Bruker APEX II  
53  
54 single crystal X-ray diffractometer, Mo-radiation. Crystal-to-detector distance was 40 mm and  
55  
56 exposure time was 15 seconds per frame for all sets. The scan width was 0.5°. Data collection  
57  
58  
59  
60

1  
2  
3 was 99.9% complete to 25° in  $\theta$ . A total of 113483 reflections were collected covering the  
4  
5 indices,  $h = -11$  to 11,  $k = -38$  to 38,  $l = -18$  to 18. 16915 reflections were symmetry independent  
6  
7 and the  $R_{\text{int}} = 0.0703$  indicated that the data was of average quality (0.07). Indexing and unit cell  
8  
9 refinement indicated a primitive monoclinic lattice. The space group was found to be  $P 2_1$  (No.4).  
10  
11 The data were integrated and scaled using SAINT, SADABS within the APEX2 software  
12  
13 package by Bruker.<sup>30</sup> Solution by direct methods (SHELXS, SIR97)<sup>31, 32</sup> produced a complete  
14  
15 heavy atom phasing model consistent with the proposed structure. The structure was completed  
16  
17 by difference Fourier synthesis with SHELXL97.<sup>33, 34</sup> Scattering factors are from Waasmair and  
18  
19 Kirfel.<sup>35</sup> Hydrogen atoms were placed in geometrically idealised positions and constrained to  
20  
21 ride on their parent atoms with C---H distances in the range 0.95-1.00 Angstrom. Isotropic  
22  
23 thermal parameters  $U_{\text{eq}}$  were fixed such that they were  $1.2U_{\text{eq}}$  of their parent atom  $U_{\text{eq}}$  for CH's  
24  
25 and  $1.5U_{\text{eq}}$  of their parent atom  $U_{\text{eq}}$  in case of methyl groups. All non-hydrogen atoms were  
26  
27 refined anisotropically by full-matrix least-squares.  
28  
29  
30  
31  
32

33  
34 *PfDHODH Crystallization, data collection, structure determination and refinement for the*  
35  
36 *PfDHODH-13 bound structure.*  
37

38  
39 Preliminary crystallization conditions were found using the random crystallization screen  
40  
41 *Cryos* suite (Nextal). Then the condition was refined by variation of pH, precipitant, and protein  
42  
43 concentrations to find optimal conditions. Crystallization was setup with hanging drop vapor  
44  
45 diffusion at 20°C. Crystals of *PfDHODH* <sub>$\Delta$ 384-413</sub>-**13** complex grew at condition with 0.16 M  
46  
47 Ammonium sulfate, 0.1 M NaAcetate, pH 4.2, 9.5% PEG4000 (w/v), 24% Glycerol (v/v), and 10  
48  
49 mM DTT. The crystallization drop was mixed with an equal volume of reservoir solution and  
50  
51 *PfDHODH* <sub>$\Delta$ 384-413</sub> (27 mg/ml) pre-equilibrated with 1 mM **13** (0.1 M stock solution in DMSO)  
52  
53  
54  
55  
56  
57  
58  
59  
60

1  
2  
3 and 2 mM dihydroorotate (DHO, 0.1 M stock solution in DMSO). All commercially available  
4 reagents were obtained from Sigma. Crystals typically grew in 1 week.  
5  
6  
7

8  
9 Diffraction data were collected at 100K on beamline 19ID at Advanced Photon Source (APS)  
10 using an ADSC Q315 detector. The crystal of *Pf*DHODH $_{\Delta 384-413}$ -13 diffracted to 2.32 Å and has  
11 a space group of P6<sub>4</sub> with the cell dimension of a=b=86.1, c=139.1 (Table S3). The structure  
12 contains only one molecule of *Pf*DHODH in the asymmetric unit. Diffraction data were  
13 integrated and intensities were scaled with HKL2000 package.<sup>36</sup>  
14  
15  
16  
17  
18  
19

20  
21 Crystallographic phases for *Pf*DHODH inhibitors were solved by molecular replacement  
22 with Phaser<sup>37</sup> using the previously reported structure of *Pf*DHODH $_{\Delta 384-413}$  bound to **DSM1** (PDB  
23 ID 3I65<sup>17</sup>) as a search model (ligands were removed from the search model). Structures were  
24 rebuilt with COOT<sup>38</sup> and refined in PHENIX<sup>39</sup> to R<sub>work</sub> and R<sub>free</sub> of 0.18 and 0.21 respectively  
25 (Table S3). Electron density for residues 159-160, 344-354, 567-569 were missing and thus not  
26 built into the final structure. The final structure contained 2972 atoms and 73 water molecules.  
27  
28 Atomic representations were created using PyMOL Molecular Graphics System (Version 1.7,  
29 Schrödinger).  
30  
31  
32  
33  
34  
35  
36  
37  
38  
39

#### 40 41 *Chemistry General Methods.* 42

43  
44 All reagents and starting materials were obtained from commercial suppliers and used  
45 without further purification unless otherwise stated. Reaction progress was monitored by thin  
46 layer chromatography (TLC) on preloaded silica gel 60 F<sub>254</sub> plates. Visualization was achieved  
47 with UV light and iodine vapor. Flash chromatography was carried out using prepacked  
48 Teledyne Isco Redisep Rf silica-gel columns as the stationary phase and analytical grade  
49 solvents as the eluent unless otherwise stated. Yields were of purified product and were not  
50  
51  
52  
53  
54  
55  
56  
57  
58  
59  
60

1  
2  
3 optimized.  $^1\text{H}$  NMR spectra were recorded on Bruker Avance 300 and 500 MHz spectrometer at  
4 ambient temperature. Chemical shifts are reported in parts per million ( $\delta$ ) and coupling constants  
5 in Hz.  $^1\text{H}$  NMR spectra were referenced to the residual solvent peaks as internal standards (7.26  
6 ppm for  $\text{CDCl}_3$ , 2.50 ppm for  $\text{DMSO-}d_6$ , and 3.34 ppm for MeOD). Spin multiplicities are  
7 described as s (singlet), brs (broad singlet), d (doublet), t (triplet), q (quartet), dd (doublet of  
8 doublets), dt (doublet of triplets) and m (multiplet). Total ion current traces were obtained for  
9 electrospray positive and negative ionization (ES+/ES-) on a Bruker Esquire Liquid  
10 Chromatograph-Ion trap mass spectrometer. Analytical chromatographic conditions used for the  
11 LC/MS analysis: Column, Zorbax Extend C18 from Agilent technologies, 2.1x100 mm. The  
12 stationary phase particle size is 3.5 $\mu\text{M}$ . Solvents were A, aqueous solvent = water +5%  
13 acetonitrile+1% acetic acid; B, organic solvent = acetonitrile + 1% acetic acid; Methods, 14 min  
14 run time (0-10 min 20-100% B, flow rate-0.275 mL/min; 10-12 min 100% B, flow rate-0.350  
15 mL/min; 12-12.50 min 100-20% B, flow rate-0.350 mL/min; 12.50-14.0 min 20% B, flow rate-  
16 0.350 mL/min). The following additional parameters were used: injection volume (10  $\mu\text{L}$ ),  
17 column temperature (30  $^\circ\text{C}$ ), UV wavelength range (254-330 nm). Analytical HPLC analyses  
18 were performed on a SupelcoSIL LC18 column (5  $\mu\text{m}$ , 4.6mm x 25cm) with a linear elution  
19 gradient ranging from 0-100% ACN over 27 min, using a SupelcoSIL LC18 column (5  $\mu\text{m}$ ,  
20 4.6mm x 25cm) at a flow rate of 1 mL/min. A purity of >95% has been established for all  
21 reported compounds (Table 1). The two enantiomers were separated for selected compounds on  
22 a semi-preparative chiral HPLC on Chiralcel OD-H (250 x 20) mm column eluting with 0.1%  
23 Diethylamine in hexane (A):Ethanol (B) 36 min run time (0-10 min, 20% B; 10-20 min, 20-35%  
24 B; 20-30 min, 35% B; 30.01-36 min 20% B; flow rate: 5 mL/min).

### 25 26 27 28 29 30 31 32 33 34 35 36 37 38 39 40 41 42 43 44 45 46 47 48 49 50 51 52 53 54 55 56 57 58 59 60 *Experimental Data*

1  
2  
3  
4  
5  
6  
7  
8  
9  
10  
11  
12  
13  
14  
15  
16  
17  
18  
19  
20  
21  
22  
23  
24  
25  
26  
27  
28  
29  
30  
31  
32  
33  
34  
35  
36  
37  
38  
39  
40  
41  
42  
43  
44  
45  
46  
47  
48  
49  
50  
51  
52  
53  
54  
55  
56  
57  
58  
59  
60

**2-(1,1-Difluoroethyl)-5-methyl-N-(1,2,3,4-tetrahydronaphthalen-2-yl)-[1,2,4]triazolo[1,5-a]pyrimidin-7-amine (5)** White solid (89% yield).  $^1\text{H}$  NMR (400 MHz,  $\text{DMSO-}d_6$ )  $\delta$  ppm: 8.24 (d,  $J = 7.1$  Hz, 1H), 7.13- 7.09 (m, 4H), 6.67 (s, 1H), 4.16 - 4.01 (br, 1H), 3.10 - 3.04 (m, 2H), 3.02 - 2.85 (m, 2H), 2.45 (s, 3H), 2.15 - 2.06 (m, 4H), 2.04 - 1.91 (m, 1H); ESIMS  $m/z$  344 (MH) $^+$ .

**2-(1,1-Difluoroethyl)-N-(6-fluoro-1,2,3,4-tetrahydronaphthalen-2-yl)-5-methyl-[1,2,4]triazolo[1,5-a]pyrimidin-7-amine (6)** White solid (75% yield).  $^1\text{H}$  NMR (500 MHz,  $\text{DMSO-}d_6$ )  $\delta$  8.29 (d,  $J = 8.8$  Hz, 1H), 7.28 - 7.07 (m, 1H), 7.06 - 6.88 (m, 2H), 6.69 (s, 1H), 4.17 - 3.94 (m, 1H), 3.14 - 2.92 (m, 4H), 2.47 (s, 3H), 2.12 (t,  $J = 18.8$ , 3H), 2.03 - 1.90 (m, 2H). ESIMS  $m/z$ : 362.1(MH) $^+$ .

**2-(1,1-Difluoroethyl)-N-(6-chloro-1,2,3,4-tetrahydronaphthalen-2-yl)-5-methyl-[1,2,4]triazolo[1,5-a]pyrimidin-7-amine (7) (Enantiomer-I):** White solid.  $^1\text{H}$  NMR (400 MHz, MeOD):  $\delta$  7.17 - 7.12 (m, 3H), 6.55 (s, 1H), 4.15 - 4.13 (m, 1H), 3.26 - 3.20 (m, 1H), 3.05 - 2.94 (m, 3H), 2.55 (s, 3H), 2.29 - 2.25 (m, 1H), 2.11 (t,  $J = 18.72$  Hz, 3H), 2.01 - 1.97 (m, 1H). ESIMS  $m/z$ : 378 (MH) $^+$ .

**2-(1,1-Difluoroethyl)-N-(6-chloro-1,2,3,4-tetrahydronaphthalen-2-yl)-5-methyl-[1,2,4]triazolo[1,5-a]pyrimidin-7-amine (8) (Enantiomer-II):** White solid.  $^1\text{H}$  NMR (400 MHz, MeOD):  $\delta$  7.17 - 7.12 (m, 3H), 6.55 (s, 1H), 4.18 - 4.12 (m, 1H), 3.26 - 3.21 (m, 1H), 3.05 - 2.95 (m, 3H), 2.55 (s, 3H), 2.29 - 2.25 (m, 1H), 2.11 (t,  $J = 18.72$  Hz, 3H), 2.01 - 1.95 (m, 1H). ESIMS  $m/z$ : 378 (MH) $^+$ .

**(S)-N-(7-Chloro-1,2,3,4-tetrahydronaphthalen-2-yl)-2-(1,1-difluoroethyl)-5-methyl-[1,2,4]triazolo[1,5-a]pyrimidin-7-amine (9) (Enantiomer-I):** White solid.  $^1\text{H}$  NMR (400 MHz,

1  
2  
3 MeOD):  $\delta$  7.16 – 7.13 (m, 3H), 6.55 (s, 1H), 4.15 – 4.12 (m, 1H), 3.26 – 3.21 (m, 1H), 3.01 –  
4  
5 2.97 (m, 3H), 2.55 (s, 3H), 2.29 – 2.25 (m, 1H), 2.11 (t,  $J = 18.75$  Hz, 3H), 2.01 – 1.94 (m, 1H).  
6  
7

8 ESIMS m/z: 378(MH)<sup>+</sup>.  
9

10 **(R)-N-(7-Chloro-1,2,3,4-tetrahydronaphthalen-2-yl)-2-(1,1-difluoroethyl)-5-methyl-**

11 **[1,2,4]triazolo[1,5-a]pyrimidin-7-amine (10) (Enantiomer-II):** White solid. <sup>1</sup>H NMR (400  
12  
13 MHz, MeOD):  $\delta$  7.16 – 7.13 (m, 3H), 6.55 (s, 1H), 4.16 – 4.12 (m, 1H), 3.26 – 3.21 (m, 1H),  
14  
15 3.03 – 2.97 (m, 3H), 2.55 (s, 3H), 2.29 – 2.25 (m, 1H), 2.11 (t,  $J = 18.72$  Hz, 3H), 2.01 – 1.95  
16  
17 (m, 1H). ESIMS m/z: 378(MH)<sup>+</sup>.  
18  
19  
20  
21

22 **2-(1,1-Difluoroethyl)-N-(6-bromo-1,2,3,4-tetrahydronaphthalen-2-yl)-5-methyl-**

23 **[1,2,4]triazolo[1,5-a]pyrimidin-7-amine (11) (Enantiomer-I is the second eluted on the**  
24  
25 **chiral column) :** White solid. <sup>1</sup>H NMR (400 MHz, CDCl<sub>3</sub>):  $\delta$  7.32 – 7.30 (m, 2H), 6.99 (d,  $J =$   
26  
27 8.04 Hz, 1H), 6.17 (d,  $J = 8.32$  Hz, 1H), 6.14 (s, 1H), 4.02 – 3.99 (m, 1H), 3.29 – 3.23 (m, 1H),  
28  
29 3.02 – 2.99 (m, 2H), 2.91 – 2.84 (m, 1H), 2.60 (s, 3H), 2.31 – 2.28 (m, 1H), 2.15 (t,  $J = 18.76$ Hz,  
30  
31 3H), 1.99 – 1.94 (m, 1H). ESIMS m/z: 424 (M+2)  
32  
33  
34  
35

36 **2-(1,1-Difluoroethyl)-N-(6-bromo-1,2,3,4-tetrahydronaphthalen-2-yl)-5-methyl-**

37 **[1,2,4]triazolo[1,5-a]pyrimidin-7-amine (12) (Enantiomer-II is the first eluted on the chiral**  
38  
39 **column):** White solid. <sup>1</sup>H NMR (400 MHz, CDCl<sub>3</sub>):  $\delta$  7.32 – 7.29 (m, 2H), 6.99 (d,  $J = 8.04$  Hz,  
40  
41 1H), 6.18 (d,  $J = 7.56$  Hz, 1H), 6.15 (s, 1H), 4.01 (brs, 1H), 3.29 – 3.24 (m, 1H), 3.02 – 2.99 (m,  
42  
43 2H), 2.91 – 2.85 (m, 1H), 2.60 (s, 3H), 2.31 – 2.29 (m, 1H), 2.15 (t,  $J = 18.76$ Hz, 3H), 1.99 –  
44  
45 1.95 (m, 1H). ESIMS m/z: 424 (M+2).  
46  
47  
48  
49

50 **2-(1,1-Difluoroethyl)-N-(7-bromo-1,2,3,4-tetrahydronaphthalen-2-yl)-5-methyl-**

51 **[1,2,4]triazolo[1,5-a]pyrimidin-7-amine (13) (Enantiomer-I)** White solid. <sup>1</sup>H NMR (400  
52  
53 MHz, DMSO-*d*<sub>6</sub>):  $\delta$  8.28 (d,  $J = 8.76$  Hz, 1H), 7.34 – 7.30 (m, 2H), 7.11 (d,  $J = 8.00$  Hz, 1H),  
54  
55  
56  
57  
58  
59  
60

6.67 (s, 1H), 4.07 (brs, 1H), 3.09 – 3.05 (m, 2H), 2.93 – 2.89 (m, 2H), 2.45 (s, 3H), 2.29 – 2.25 (m, 1H), 2.11 (t,  $J = 19.12$  Hz, 3H), 1.98 – 1.94 (m, 1H). ESIMS  $m/z$ : 422 (MH)<sup>+</sup>.

**2-(1,1-Difluoroethyl)-N-(7-bromo-1,2,3,4-tetrahydronaphthalen-2-yl)-5-methyl-**

**[1,2,4]triazolo[1,5-a]pyrimidin-7-amine (14) (Enantiomer-II)** : White solid. <sup>1</sup>H NMR (400 MHz, DMSO-*d*<sub>6</sub>):  $\delta$  8.28 (d,  $J = 8.00$  Hz, 1H), 7.34 – 7.30 (m, 2H), 7.11 (d,  $J = 8.16$  Hz, 1H), 6.68 (s, 1H), 4.07 (brs, 1H) 3.09 – 3.05 (m, 2H), 2.90 – 2.88 (m, 2H), 2.45 (s, 3H), 2.29 – 2.25 (m, 1H), 2.11 (t,  $J = 19.02$  Hz, 3H), 1.98 – 1.94 (m, 1H). ESIMS  $m/z$ : 424 (M+2).

**2-(1,1-Difluoroethyl)-N-(6-methoxy-1,2,3,4-tetrahydronaphthalen-2-yl)-5-methyl-**

**[1,2,4]triazolo[1,5-a]pyrimidin-7-amine (15)** White solid (85% yield). <sup>1</sup>H NMR (300 MHz, CDCl<sub>3</sub>)  $\delta$  7.06 (d,  $J = 8.3$  Hz, 1H), 6.86 – 6.63 (m, 2H), 6.31 – 6.07 (m, 2H), 4.15 – 3.92 (m, 1H), 3.82 (s, 3H), 3.27 (dd,  $J = 15.7, 4.2$  Hz, 1H), 3.13 – 2.79 (m, 3H), 2.61 (s, 3H), 2.44 – 2.24 (m, 1H), 2.16 (t,  $J = 18.8$  Hz, 3H), 2.07 – 1.88 (m, 1H). ESIMS  $m/z$ : 374.4 (MH)<sup>+</sup>.

**2-(1,1-Difluoroethyl)-N-(7-methoxy-1,2,3,4-tetrahydronaphthal-en-2-yl)-5-methyl-**

**[1,2,4]triazolo[1,5-a]pyrimidin-7-amine (16) (Enantiomer-I):**

<sup>1</sup>H NMR (400 MHz, MeOD):  $\delta$  7.05 (d,  $J = 8.4$ , 1H), 6.75 – 6.55 (m, 2H), 6.55 (s, 1H), 4.15 – 4.12 (m, 1H), 3.76 (s, 3H), 3.25 – 3.19 (m, 1H), 3.01 – 2.94 (m, 3H), 2.56 (s, 3H), 2.28 – 2.25 (m, 1H), 2.11 (t,  $J = 18.75$  Hz, 3H), 2.16 – 1.94 (m, 1H). ESI-MS  $m/z$ : 374.2(MH)<sup>+</sup>.

**2-(1,1-Difluoroethyl)-N-(7-methoxy-1,2,3,4-tetrahydronaphthal-en-2-yl)-5-methyl-**

**[1,2,4]triazolo[1,5-a]pyrimidin-7-amine (17) (Enantiomer-II):** White solid. <sup>1</sup>H NMR (400 MHz, MeOD):  $\delta$  7.05 (d,  $J = 8.4$ , 1H), 6.75 – 6.69 (m, 2H), 6.55 (s, 1H), 4.14 – 4.12 (m, 1H), 3.76 (s, 3H), 3.25 – 3.19 (m, 1H), 3.01 – 2.94 (m, 3H), 2.56 (s, 3H), 2.28 – 2.24 (m, 1H), 2.14 (t,  $J = 18.68$  Hz, 3H), 2.03 – 1.96 (m, 1H). ESI-MS  $m/z$ : 374.2(MH)<sup>+</sup>.

1  
2  
3  
4  
5  
6  
7  
8  
9  
10  
11  
12  
13  
14  
15  
16  
17  
18  
19  
20  
21  
22  
23  
24  
25  
26  
27  
28  
29  
30  
31  
32  
33  
34  
35  
36  
37  
38  
39  
40  
41  
42  
43  
44  
45  
46  
47  
48  
49  
50  
51  
52  
53  
54  
55  
56  
57  
58  
59  
60

**2-(1,1-Difluoroethyl)-N-(6,7-difluoro-1,2,3,4-tetrahydronaphthalen-2-yl)-5-methyl-[1,2,4]triazolo[1,5-a]pyrimidin-7-amine (18) (Enantiomer-I)** White solid.  $^1\text{H}$  NMR (500 MHz,  $\text{CDCl}_3$ )  $\delta$  7.05 – 6.92 (m, 2H), 6.43 – 6.25 (m, 2H), 4.13 – 3.97 (m, 1H), 3.36 – 3.16 (m, 1H), 3.12 – 2.85 (m, 3H), 2.64 (s, 3H), 2.43 – 2.28 (m, 1H), 2.16 (t,  $J = 18.92$  Hz, 3H), 2.08 – 1.91 (m, 1H). ESIMS  $m/z$ : 380.2 (MH) $^+$ .

**2-(1,1-Difluoroethyl)-N-(6,7-difluoro-1,2,3,4-tetrahydronaphthalen-2-yl)-5-methyl-[1,2,4]triazolo[1,5-a]pyrimidin-7-amine (19) (Enantiomer-II)** White solid.  $^1\text{H}$  NMR (300 MHz,  $\text{CDCl}_3$ )  $\delta$  7.08 – 6.86 (m, 2H), 6.26 – 6.13 (s, 2H), 4.13 – 3.93 (m, 1H), 3.33 – 3.20 (m, 1H), 3.11 – 2.83 (m, 3H), 2.63 (s, 3H), 2.38 – 2.25 (m, 1H), 2.08 (t,  $J = 18.8$  Hz, 3H), 2.06 – 1.89 (m, 1H). ESIMS  $m/z$ : 380.2 (MH) $^+$ .

**2-(1,1-Difluoroethyl)-N-(6-fluoro-7-(trifluoromethyl)-1,2,3,4-tetrahydronaphthalen-2-yl)-5-methyl-[1,2,4]triazolo[1,5-a]pyrimidin-7-amine (20)** White solid (80% yield)  $^1\text{H}$  NMR (500 MHz,  $\text{CDCl}_3$ )  $\delta$  7.39 (d,  $J = 7.0$  Hz, 1H), 7.04 (d,  $J = 10.8$  Hz, 1H), 6.36 – 6.06 (m, 2H), 4.11 – 4.01 (m, 1H), 3.35 (dd,  $J = 16.2, 4.7$  Hz, 1H), 3.18 – 2.92 (m, 3H), 2.63 (s, 3H), 2.43 – 2.31 (m, 1H), 2.17 (t,  $J = 18.8$  Hz, 3H), 2.06 – 1.95 (m, 1H). ESIMS  $m/z$ : 430.2 (MH) $^+$ .

**2-(1,1-Difluoroethyl)-N-(7-fluoro-6-(trifluoromethyl)-1,2,3,4-tetrahydro-naphthalen-2-yl)-5-methyl-[1,2,4]triazolo[1,5-a]pyrimidin-7-amine (21)** White solid (83% yield)  $^1\text{H}$  NMR (300 MHz,  $\text{CDCl}_3$ )  $\delta$  7.42 (d,  $J = 7.0$  Hz, 1H), 6.99 (d,  $J = 10.6$  Hz, 1H), 6.26 – 6.10 (m, 2H), 4.10 – 3.98 (m, 1H), 3.37 (dd,  $J = 16.9, 4.9$  Hz, 1H), 3.15 – 2.89 (m, 3H), 2.64 (s, 3H), 2.47 – 2.28 (m, 1H), 2.16 (t,  $J = 18.8$  Hz, 3H), 2.05 – 1.95 (m, 1H). ESIMS  $m/z$ : 452.3 (M+Na) $^+$ .

**5-Methyl-N-(1,2,3,4-tetrahydronaphthalen-2-yl)-2-(trifluoromethyl)-[1,2,4]triazolo[1,5-a]pyrimidin-7-amine (22)** White solid (90% yield).  $^1\text{H}$  NMR (300 MHz,  $\text{CDCl}_3$ )  $\delta$  (ppm): 7.25

1  
2  
3  
4  
5  
6  
7  
8  
9  
– 7.09 (m, 4H), 6.23 (s, 1H), 6.17 (d,  $J = 8.0$  Hz, 1H), 4.15 – 3.98 (m, 1H), 3.35 (dd,  $J = 16.4$ ,  
5.0 Hz, 1H), 3.15 – 2.84 (m, 3H), 2.64 (s, 3H), 2.41 – 2.26 (m, 1H), 2.12 – 1.95 (m, 1H); ESIMS  
 $m/z$ : 348.3 (MH)<sup>+</sup>.

10  
11  
12  
13  
14  
15  
16  
17  
18  
19  
20  
21  
22  
23  
24  
**N-(6-Fluoro-1,2,3,4-tetrahydronaphthalen-2-yl)-5-methyl-2-(trifluoromethyl)-**

**[1,2,4]triazolo[1,5-a]pyrimidin-7-amine (23)** White solid (80% yield). <sup>1</sup>H NMR (500 MHz, CDCl<sub>3</sub>)  $\delta$  (ppm): 7.17 – 7.05 (m, 1H), 7.0 – 6.82 (m, 2H), 6.43 – 6.12 (m, 2H), 4.12 – 3.99 (m, 1H), 3.37 – 3.26 (m, 1H), 3.10 – 2.89 (m, 3H), 2.64 (s, 3H), 2.40 – 2.29 (m, 1H), 2.09 – 1.98 (m, 1H). ESIMS  $m/z$ : 366.3(MH)<sup>+</sup>.

25  
26  
27  
28  
29  
30  
31  
32  
33  
34  
35  
36  
37  
38  
39  
40  
41  
42  
43  
44  
45  
46  
47  
48  
49  
50  
51  
52  
53  
54  
55  
**N-(7-Chloro-1,2,3,4-tetrahydronaphthalen-2-yl)-5-methyl-2-(trifluoromethyl)-**

**[1,2,4]triazolo[1,5-a]pyrimidin-7-amine (24) (Enantiomer-I)** <sup>1</sup>H NMR (400 MHz, MeOD)  $\delta$  (ppm): 7.17 – 7.10 (m, 3H), 6.62 (s, 1H), 4.19 – 4.09 (m, 1H), 3.27 – 3.19 (m, 1H), 3.05 – 2.90 (m, 3H), 2.56 (s, 3H), 2.30 – 2.20 (m, 1H), 2.05 – 1.94 (m, 1H). ESIMS  $m/z$ : 382.2(MH)<sup>+</sup>

56  
57  
58  
59  
60  
**N-(7-Chloro-1,2,3,4-tetrahydronaphthalen-2-yl)-5-methyl-2-(trifluoromethyl)-**

**[1,2,4]triazolo[1,5-a]pyrimidin-7-amine (25) (Enantiomer-II)** <sup>1</sup>H NMR (400 MHz, MeOD)  $\delta$  (ppm): 7.17 – 7.10 (m, 3H), 6.62 (s, 1H), 4.18 – 4.10 (m, 1H), 3.27 – 3.19 (m, 1H), 3.05 – 2.90 (m, 3H), 2.56 (s, 3H), 2.30 – 2.20 (m, 1H), 2.05 – 1.97 (m, 1H). ESIMS  $m/z$ : 382.0(MH)<sup>+</sup>

**2-(1,1-Difluoroethyl)-N-(2,3-dihydro-1H-inden-2-yl)-5-methyl[1,2,4]triazolo[1,5-a]pyrim-**

**idin-7-amine (26)** pale yellow solid (85% yield). <sup>1</sup>H NMR (400 MHz, CDCl<sub>3</sub>)  $\delta$  ppm: 7.30 – 7.24 (m, 4H), 6.3 (d,  $J = 7.3$  Hz, 1H), 6.18 (s, 1H), 4.57 – 4.49 (m, 1H), 3.51 (dd,  $J = 7.1$  Hz,  $J = 16.2$  Hz, 2H), 3.13 – 3.08 (m, 2H), 2.62 (s, 3H), 2.13 (t,  $J = 18.7$  Hz, 3H); ESIMS  $m/z$  330 (MH)<sup>+</sup>.

**N-(5-Bromo-2,3-dihydro-1H-inden-2-yl)-2-(1,1-difluoroethyl)-5-methyl-[1,2,4]triazolo[1,5-a]pyrimidin-7-amine (27)** White foam (57% yield). <sup>1</sup>H NMR (400 MHz, DMSO-*d*<sub>6</sub>)  $\delta$  ppm:

1  
2  
3 8.55 – 8.49 (br, 1H), 7.46 – 7.44 (br, 1H), 7.37 – 7.35 (m, 1H), 7.22 – 7.20 (m, 1H), 6.63 (s, 1H),  
4  
5 4.68 – 4.58 (br, 1H), 3.32 – 3.28 (br, 1H), 3.21 – 3.12 (m, 3H), 2.47 (s, 3H), 2.09 (t,  $J = 19.2$  Hz,  
6  
7 3H); ESIMS  $m/z$  408 (MH)<sup>+</sup>.  
8  
9

10 **N-(5-Chloro-2,3-dihydro-1H-inden-2-yl)-2-(1,1-difluoroethyl)-5-methyl-[1,2,4] triazolo[1,5-**  
11 **a]pyrimidin-7-amine (28)** White solid (82% yield). <sup>1</sup>H NMR (400 MHz, DMSO-*d*<sub>6</sub>)  $\delta$  ppm:  
12  
13 8.57 – 8.48 (m, 1 H), 7.34 – 7.29 (m, 1 H), 7.29 – 7.19 (m, 2 H), 6.63 (s, 1 H), 4.72 – 4.57 (m, 1  
14  
15 H), 3.41 – 3.35 (m, 2 H), 3.23 – 3.07 (m, 2 H), 2.09 (t,  $J = 19.1$  Hz, 3 H); ESIMS  $m/z$  364  
16  
17 (MH)<sup>+</sup>.  
18  
19

20 **N-(5,6-Dichloro-2,3-dihydro-1H-inden-2-yl)-2-(1,1-difluoroethyl)-5-methyl-**  
21 **[1,2,4]triazolo[1,5-a]pyrimidin-7-amine (29)** White solid (41% yield). <sup>1</sup>H NMR (400 MHz,  
22  
23 CDCl<sub>3</sub>)  $\delta$  ppm: 7.37 (s, 2H), 6.28 (d,  $J = 7.6$  Hz, 1H), 6.16 (s, 1H), 4.60 – 4.52 (m, 1H), 3.51 –  
24  
25 3.45 (m, 2H), 3.07 (dd,  $J = 4.5$  Hz,  $J = 16.4$  Hz, 2H), 2.62 (s, 3H), 2.13 (t,  $J = 18.7$  Hz, 3H);  
26  
27 ESIMS  $m/z$  398 (MH)<sup>+</sup>.  
28  
29

30 **2-(1,1-Difluoroethyl)-5-methyl-N-(5-(methylsulfonyl)-2,3-dihydro-1H-inden-2-yl)-**  
31 **[1,2,4]triazolo[1,5-a]pyrimidin-7-amine (30)** White solid (58% yield). <sup>1</sup>H NMR (400 MHz,  
32  
33 DMSO-*d*<sub>6</sub>)  $\delta$  ppm: 8.57 (d,  $J = 7.6$  Hz, 1 H), 7.82 – 7.78 (m, 1 H), 7.78 – 7.69 (m, 1 H), 7.57 –  
34  
35 7.47 (m, 1 H), 6.65 (s, 1 H), 4.79 – 4.63 (m, 1 H), 3.52 – 3.38 (m, 2 H), 3.30 – 3.18 (m, 2H), 3.19  
36  
37 (s, 3 H), 2.48 (s, 3 H), 2.09 (t,  $J = 19.2$  Hz, 3 H); ESIMS  $m/z$  408 (MH)<sup>+</sup>.  
38  
39

40 **2-(2-(1,1-Difluoroethyl)-5-methyl-[1,2,4]triazolo[1,5-a]pyrimidin-7-ylamino)-N,N-dimethyl-**  
41 **2,3-dihydro-1H-indene-5-sulfonamide (31)** White solid (62% yield). <sup>1</sup>H NMR (400 MHz,  
42  
43 DMSO-*d*<sub>6</sub>)  $\delta$  ppm: 8.59 (d,  $J = 7.8$  Hz, 1 H), 7.61 (br s, 1 H), 7.60 – 7.54 (m, 1 H), 7.53 – 7.48  
44  
45 (m, 1 H), 6.65 (s, 1 H), 4.76 – 4.64 (m, 1 H), 3.52 – 3.39 (m, 2 H), 3.30 – 3.19 (m, 2 H), 2.61 (s,  
46  
47 6 H), 2.48 (s, 3 H), 2.09 (t,  $J = 19.2$  Hz, 3 H); ESIMS  $m/z$  437 (MH)<sup>+</sup>.  
48  
49  
50  
51  
52  
53  
54  
55  
56  
57  
58  
59  
60

**N-(4,7-Dimethyl-2,3-dihydro-1H-inden-2-yl)-2-(1,1-difluoroethyl)-5-methyl-**

**[1,2,4]triazolo[1,5-a]pyrimidin-7-amine (32)** White solid (74% yield). <sup>1</sup>H NMR (400 MHz, CDCl<sub>3</sub>) δ ppm: 6.99 (s, 2H), 6.31 (d, *J* = 7.6 Hz, 1H), 6.19 (s, 1H), 4.58 – 4.50 (m, 1H), 3.45 (dd, *J* = 7.3 Hz, *J* = 16.2 Hz, 2H), 3.05 – 2.99 (m, 2H), 2.63 (s, 3H), 2.26 (s, 6H), 2.14 (t, *J* = 18.7 Hz, 3H); ESIMS *m/z* 358 (MH)<sup>+</sup>.

**N-(4,7-Difluoro-2,3-dihydro-1H-inden-2-yl)-2-(1,1-difluoroethyl)-5-methyl-[1,2,4]**

**triazolo[1,5-a]pyrimidin-7-amine (33)** White solid (65% yield). <sup>1</sup>H NMR (300 MHz, CDCl<sub>3</sub>) δ 6.94 (t, *J* = 5.8 Hz, 2H), 6.42 (brs, 1H), 6.21 (s, 1H), 4.73 – 4.53 (m, 1H), 3.70 – 3.44 (m, 2H), 3.35 – 3.08 (m, 2H), 2.67 (s, 3H), 2.14 (t, *J* = 18.8 Hz, 3H). ESIMS *m/z*: 366.3 (MH)<sup>+</sup>.

**2-(1,1-Difluoroethyl)-N-(4-fluoro-2,3-dihydro-1H-inden-2-yl)-5-methyl-[1,2,4]triazolo[1,5-**

**a]pyrimidin-7-amine (34)** White solid (58% yield). <sup>1</sup>H NMR (300 MHz, CDCl<sub>3</sub>) δ 7.24 (dd, *J* = 8.1, 5.2 Hz, 1H), 7.04 – 6.88 (m, 2H), 6.33 (d, *J* = 7.3 Hz, 1H), 6.19 (s, 1H), 4.68 – 4.48 (m, 1H), 3.50 (dt, *J* = 15.4, 7.7 Hz, 2H), 3.20 – 3.00 (m, 2H), 2.63 (s, 3H), 2.15 (t, *J* = 18.8 Hz, 3H). ESIMS *m/z*: 348.5 (MH)<sup>+</sup>.

**N-(5,6-Difluoro-2,3-dihydro-1H-inden-2-yl)-2-(1,1-difluoroethyl)-5-methyl-[1,2,4]**

**triazolo[1,5-a]pyrimidin-7-amine (35)** White solid (75% yield). <sup>1</sup>H NMR (500 MHz, CDCl<sub>3</sub>) δ 7.10 (t, *J* = 8.6 Hz, 2H), 6.31 (d, *J* = 7.5 Hz, 1H), 6.18 (s, 1H), 4.71 – 4.48 (m, 1H), 3.50 (dd, *J* = 16.2, 7.0 Hz, 2H), 3.17 – 2.97 (m, 2H), 2.64 (s, 3H), 2.16 (t, *J* = 18.8 Hz, 3H). ESIMS *m/z*: 366.3(MH)<sup>+</sup>.

**2-(1,1-Difluoroethyl)-5-methyl-N-(4-(trifluoromethyl)-2,3-dihydro-1H-inden-2-yl)-**

**[1,2,4]triazolo[1,5-a]pyrimidin-7-amine (36)** White solid (70% yield). <sup>1</sup>H NMR (500 MHz, CDCl<sub>3</sub>) δ 7.56 (d, *J* = 7.8 Hz, 1H), 7.50 (d, *J* = 7.5 Hz, 1H), 7.40 (t, *J* = 7.7 Hz, 1H), 6.32 (d, *J* = 7.4 Hz, 1H), 6.22 (s, 1H), 4.71 – 4.57 (m, 1H), 3.71 (dd, *J* = 17.2, 7.2 Hz, 1H), 3.60 (dd, *J* =

1  
2  
3 16.5, 7.3 Hz, 1H), 3.30 (dd,  $J = 17.1, 4.1$  Hz, 1H), 3.19 (dd,  $J = 16.5, 4.6$  Hz, 1H), 2.66 (s, 3H),  
4  
5 2.16 (t,  $J = 18.8$  Hz, 3H). ESIMS  $m/z$ : 398.3(MH)<sup>+</sup>.  
6  
7

8 **N-(5,6-Difluoro-2,3-dihydro-1H-inden-2-yl)-5-methyl-2-(trifluoromethyl)-**

9  
10 **[1,2,4]triazolo[1,5-a]pyrimidin-7-amine (37)** <sup>1</sup>H NMR (400 MHz, MeOD)  $\delta$  (ppm): 7.17 (t,  $J$   
11  
12 = 9.04 Hz, 2H), 6.62 (s, 1H), 4.78 – 4.62 (m, 1H), 3.45 (dd,  $J = 16.01, 7.52$  Hz, 2H), 3.15 (dd,  $J$   
13  
14 = 15.85, 6.4 Hz, 2H), 2.59 (s, 3H). ESIMS  $m/z$ : 370.0(MH)<sup>+</sup>.  
15  
16

17 **N-(2,3-Dihydro-1H-inden-2-yl)acetamide (39)**. 2,3-dihydro-1H-inden-2-amine hydrochloride  
18  
19 **(38)** (50 g, 295 mmol), 45 mL of acetic anhydride and 25 g of sodium acetate were suspended in  
20  
21 100 mL of acetic acid and stirred overnight at r.t. The mixture was poured into 3 vols of ice-water  
22  
23 and neutralized with ammonium hydroxide. The mixture was extracted with chloroform and the  
24  
25 combined organic layers were washed with water, diluted HCl, water, dried and evaporated. The  
26  
27 residue was recrystallized from CHCl<sub>3</sub> – Et<sub>2</sub>O to yield N-(2,3-dihydro-1H-inden-2-yl)acetamide  
28  
29 **(39)** (43 g, 66 % yield).  
30  
31  
32  
33

34  
35 **2-Acetamido-2,3-dihydro-1H-indene-5-sulfonyl chloride (40)**. To a stirred, cooled solution of  
36  
37 N-(2,3-dihydro-1H-inden-2-yl)acetamide **(39)** (24.4 g, 139 mmol) in 400 mL of chloroform was  
38  
39 added dropwise 55 mL of chlorosulfonic acid below 0 °C. The solution was stirred whilst cooling  
40  
41 and then allowed to reach r.t. slowly by stirring overnight. The excess of chlorosulfonic acid  
42  
43 decomposed by adding the mixture dropwise to stirred iced water. The layers were separated and  
44  
45 the aqueous layer was extracted several times with chloroform. The chloroform layers were  
46  
47 washed, dried and evaporated. The concentrate was heated, diluted with additional chloroform,  
48  
49 but was still containing some undissolved gum. It was filtered, washed with Et<sub>2</sub>O and dried to  
50  
51 yield 2-acetamido-2,3-dihydro-1H-indene-5-sulfonyl chloride **(40)** as crystals (25.6 g, 67%  
52  
53  
54  
55  
56  
57  
58  
59  
60 yield).

1  
2  
3 **N-(5-(Methylthio)-2,3-dihydro-1H-inden-2-yl)acetamide (41).** A solution of 2-acetamido-2,3-  
4 dihydro-1H-indene-5-sulfonyl chloride (**40**) (13.7 g, 50 mmol) in 250 ml of acetic acid was  
5 stirred and warmed to 75 °C whereupon a solution of 50 g of tin (II) chloride dihydrate in 45 mL  
6 of conc. HCl was added in one portion. The solution was stirred 90-120 min at r.t. The solution  
7 was poured into several vols of water containing some conc. HCl and a yellowish-white solid  
8 precipitated. The mixture was filtered (became rapidly gummy when dried on a clay plate),  
9 washed with cold water and dissolved in 250 mL of MeOH. To the solution, under nitrogen, was  
10 added 3g of sodium methoxide in 4 mL (>0.05 mol) of methyl iodide. The mixture was stirred 2  
11 h at r.t. and left standing overnight. The mixture was concentrated and then partitioned between  
12 water and chloroform. After drying and evaporation, 8.6 g of oil were obtained which was  
13 purified by chromatography on neutral alumina eluting with EtOAc. N-(5-(methylthio)-2,3-  
14 dihydro-1H-inden-2-yl)acetamide (**41**) was obtained as a white solid after washing with Et<sub>2</sub>O and  
15 recrystallization from chloroform-Et<sub>2</sub>O (3.7 g, 33% yield).  
16  
17  
18  
19  
20  
21  
22  
23  
24  
25  
26  
27  
28  
29  
30  
31  
32  
33

34  
35 **N-(5-(Methylsulfonyl)-2,3-dihydro-1H-inden-2-yl)acetamide (42).** A solution of N-(5-  
36 (methylthio)-2,3-dihydro-1H-inden-2-yl)acetamide (**41**) (2.2 g, 9.9 mmol) and *m*-  
37 chloroperbenzoic acid (5 g) in 900 mL of chloroform was stirred at r.t. for 2h. The solution was  
38 washed with aq. 5% Na<sub>2</sub>CO<sub>3</sub>, water, dried and evaporated. The residue was triturated with Et<sub>2</sub>O,  
39 filtered and dried to yield the N-(5-(methylsulfonyl)-2,3-dihydro-1H-inden-2-yl)acetamide (**42**)  
40 as a white solid (1.87g, 75% yield).  
41  
42  
43  
44  
45  
46  
47  
48  
49

50 **5-(Methylsulfonyl)-2,3-dihydro-1H-inden-2-amine hydrochloride (43).** A mixture of 1.9 g  
51 (7.5 mmol) of N-(5-(methylsulfonyl)-2,3-dihydro-1H-inden-2-yl)acetamide (**42**) and 20 mL of  
52 3N HCl was stirred under reflux for 2.5 h. The solution was cooled and the residue was  
53  
54  
55  
56  
57  
58  
59  
60

azeotroped with EtOH. Recrystallization from MeOH-EtOH yielded 5-(methylsulfonyl)-2,3-dihydro-1H-inden-2-amine hydrochloride (**43**) as crystals (0.87g, 55% yield)

$^1\text{H}$  NMR (500 MHz, DMSO- $d_6$ )  $\delta$  8.17 (br. s., 2H), 7.84 (s, 1H), 7.79 – 7.71 (m, 1H), 7.54 (d,  $J$  = 8.0 Hz, 1H), 4.06 (ddd,  $J$  = 2.5, 5.0, 7.6 Hz, 1H), 3.40 – 3.34 (m, 2H), 3.17 (s, 3H), 3.10 – 2.98 (m, 2H). ESIMS  $m/z$ : 212.1 (MH) $^+$ .

**Supporting information.** Supporting information includes supplemental chemistry methods, supplemental tables S1 – S4 and supplemental figures S1 and S4B.

**PDB ID Codes.** Coordinates for the **13**-PfDHODH X-ray structure have been submitted to the pdb (5FI8) and coordinates for the **9** small molecule structure have been submitted to CCDC (1454120).

**Corresponding Author Information.**

Dr. Margaret A. Phillips

Department of Pharmacology

University of Texas Southwestern Medical Center at Dallas,

6001 Forest Park Blvd, Dallas, Texas 75390-9041

Phone: 214-645-6164.

Email : [margaret.phillips@UTSouthwestern.edu](mailto:margaret.phillips@UTSouthwestern.edu)

and

Dr. Pradipsinh K. Rathod

Departments of Chemistry and Global Health

University of Washington, Seattle, WA 98195

Phone: [206-221-6069](tel:206-221-6069)

1  
2  
3 Email: [rathod@chem.washington.edu](mailto:rathod@chem.washington.edu)  
4  
5

6 **Author Contributions.** SK, JMC, MM, LDLH, KM, KRR synthesized compounds described in  
7  
8 the study; SK and WK performed small molecule X-ray crystallography; XD, MAP and DT  
9  
10 performed, analyzed or supervised protein X-ray crystallography and DM contributed molecular  
11  
12 modeling insight; KW, GC, JM, ER and SAC performed, analyzed or supervised the ADME and  
13  
14 pharmacokinetic studies; FEM and MAP performed, analyzed or supervised the enzymology  
15  
16 studies; PKR, DW, JNB supervised chemistry studies; MBJ, SFB and IAB performed, analyzed  
17  
18 or supervised *in vivo* efficacy studies; SK, SAC, PKR and MAP wrote the manuscript.  
19  
20  
21

22 **Acknowledgments.** The authors would like to thank Michael Palmer for critical reading of the  
23  
24 manuscript. This work was supported by funds from the United States National Institutes of  
25  
26 Health grants, R01AI103947 (to MAP and PKR) and U01AI075594 (to IB, MAP, PKR and  
27  
28 SAC) and from Medicines for Malaria Venture (MMV). MAP acknowledges the support of the  
29  
30 Welch Foundation (I-1257). MAP holds the Beatrice and Miguel Elias Distinguished Chair in  
31  
32 Biomedical Science and the Carolyn R. Bacon Professorship in Medical Science and Education.  
33  
34

35 **Abbreviations.** DHODH, Dihydroorotate dehydrogenase; *Pf*DHODH, *P. falciparum* DHODH;  
36  
37 *Pv*DHODH, *P. vivax* DHODH, *h*DHODH, human DHODH; DSM, is the code name assigned to  
38  
39 compounds from our team and stands for Dallas, Seattle and Melbourne, reflecting the location  
40  
41 of the three project groups on the team.  
42  
43  
44  
45  
46  
47  
48  
49  
50  
51  
52  
53  
54  
55  
56  
57  
58  
59  
60

**References.**

1. WHO. World Malaria Report. <http://www.who.int/malaria/media/world-malaria-report-2015/en/> **2015**. (Access date: Feb. 1, 2016)
2. White, N. J.; Pukrittayakamee, S.; Hien, T. T.; Faiz, M. A.; Mokuolu, O. A.; Dondorp, A. M. Malaria. *Lancet* **2014**, *383*, 723-735.
3. Miller, L. H.; Ackerman, H. C.; Su, X. Z.; Wellems, T. E. Malaria biology and disease pathogenesis: insights for new treatments. *Nat. Med.* **2013**, *19*, 156-167.
4. Wells, T. N.; Hooft van Huijsduijnen, R.; Van Voorhis, W. C. Malaria medicines: a glass half full? *Nat. Rev. Drug Discovery* **2015**, *14*, 424-442.
5. Burrows, J. N.; Hooft van Huijsduijnen, R.; Mohrle, J. J.; Oeuvray, C.; Wells, T. N. Designing the next generation of medicines for malaria control and eradication. *Malar. J.* **2013**, *12*, 187. doi:10.1186/1475-2875-12-187
6. Burrows, J. N.; Chibale, K.; Wells, T. N. The state of the art in anti-malarial drug discovery and development. *Curr. Top. Med. Chem.* **2011**, *11*, 1226-1254.
7. Straimer, J.; Gnadig, N. F.; Witkowski, B.; Amaratunga, C.; Duru, V.; Ramadani, A. P.; Dacheux, M.; Khim, N.; Zhang, L.; Lam, S.; Gregory, P. D.; Urnov, F. D.; Mercereau-Puijalon, O.; Benoit-Vical, F.; Fairhurst, R. M.; Menard, D.; Fidock, D. A. Drug resistance. K13-propeller mutations confer artemisinin resistance in *Plasmodium falciparum* clinical isolates. *Science* **2015**, *347*, 428-431.
8. Mok, S.; Ashley, E. A.; Ferreira, P. E.; Zhu, L.; Lin, Z.; Yeo, T.; Chotivanich, K.; Imwong, M.; Pukrittayakamee, S.; Dhorda, M.; Nguon, C.; Lim, P.; Amaratunga, C.; Suon, S.; Hien, T. T.; Htut, Y.; Faiz, M. A.; Onyamboko, M. A.; Mayxay, M.; Newton, P. N.; Tripura, R.; Woodrow, C. J.; Miotto, O.; Kwiatkowski, D. P.; Nosten, F.; Day, N. P.; Preiser, P. R.; White,

1  
2  
3 N. J.; Dondorp, A. M.; Fairhurst, R. M.; Bozdech, Z. Drug resistance. Population transcriptomics  
4 of human malaria parasites reveals the mechanism of artemisinin resistance. *Science* **2015**, *347*,  
5 431-435.  
6  
7

8  
9  
10 9. Miotto, O.; Amato, R.; Ashley, E. A.; MacInnis, B.; Almagro-Garcia, J.; Amaratunga, C.;  
11 Lim, P.; Mead, D.; Oyola, S. O.; Dhorda, M.; Imwong, M.; Woodrow, C.; Manske, M.; Stalker,  
12 J.; Drury, E.; Campino, S.; Amenga-Etego, L.; Thanh, T. N.; Tran, H. T.; Ringwald, P.; Bethell,  
13 D.; Nosten, F.; Phyto, A. P.; Pukrittayakamee, S.; Chotivanich, K.; Chuor, C. M.; Nguon, C.;  
14 Suon, S.; Sreng, S.; Newton, P. N.; Mayxay, M.; Khanthavong, M.; Hongvanthong, B.; Htut, Y.;  
15 Han, K. T.; Kyaw, M. P.; Faiz, M. A.; Fanello, C. I.; Onyamboko, M.; Mokuolu, O. A.; Jacob, C.  
16 G.; Takala-Harrison, S.; Plowe, C. V.; Day, N. P.; Dondorp, A. M.; Spencer, C. C.; McVean, G.;  
17 Fairhurst, R. M.; White, N. J.; Kwiatkowski, D. P. Genetic architecture of artemisinin-resistant  
18 *Plasmodium falciparum*. *Nat. Genet.* **2015**, *47*, 226-234.  
19  
20  
21  
22  
23  
24  
25  
26  
27  
28  
29  
30

31 10. Burrows, J. N.; Burlot, E.; Campo, B.; Cherbuin, S.; Jeanneret, S.; Leroy, D.;  
32 Spangenberg, T.; Waterson, D.; Wells, T. N.; Willis, P. Antimalarial drug discovery - the path  
33 towards eradication. *Parasitology* **2014**, *141*, 128-139.  
34  
35  
36  
37

38 11. Coteron, J. M.; Marco, M.; Esquivias, J.; Deng, X.; White, K. L.; White, J.; Koltun, M.;  
39 El Mazouni, F.; Kokkonda, S.; Katneni, K.; Bhamidipati, R.; Shackleford, D. M.; Angulo-  
40 Barturen, I.; Ferrer, S. B.; Jimenez-Diaz, M. B.; Gamo, F. J.; Goldsmith, E. J.; Charman, W. N.;  
41 Bathurst, I.; Floyd, D.; Matthews, D.; Burrows, J. N.; Rathod, P. K.; Charman, S. A.; Phillips, M.  
42 A. Structure-guided lead optimization of triazolopyrimidine-ring substituents identifies potent  
43 *Plasmodium falciparum* dihydroorotate dehydrogenase inhibitors with clinical candidate  
44 potential. *J. Med. Chem.* **2011**, *54*, 5540-5561.  
45  
46  
47  
48  
49  
50  
51  
52  
53  
54  
55  
56  
57  
58  
59  
60

- 1  
2  
3  
4  
5  
6  
7  
8  
9  
10  
11  
12  
13  
14  
15  
16  
17  
18  
19  
20  
21  
22  
23  
24  
25  
26  
27  
28  
29  
30  
31  
32  
33  
34  
35  
36  
37  
38  
39  
40  
41  
42  
43  
44  
45  
46  
47  
48  
49  
50  
51  
52  
53  
54  
55  
56  
57  
58  
59  
60
12. Phillips, M. A.; Lotharius, J.; Marsh, K.; White, J.; Dayan, A.; White, K. L.; Njoroge, J. W.; El Mazouni, F.; Lao, Y.; Kokkonda, S.; Tomchick, D. R.; Deng, X.; Laird, T.; Bhatia, S. N.; March, S.; Ng, C. L.; Fidock, D. A.; Wittlin, S.; Lafuente-Monasterio, M.; Benito, F. J.; Alonso, L. M.; Martinez, M. S.; Jimenez-Diaz, M. B.; Bazaga, S. F.; Angulo-Barturen, I.; Haselden, J. N.; Louttit, J.; Cui, Y.; Sridhar, A.; Zeeman, A. M.; Kocken, C.; Sauerwein, R.; Dechering, K.; Avery, V. M.; Duffy, S.; Delves, M.; Sinden, R.; Ruecker, A.; Wickham, K. S.; Rochford, R.; Gahagen, J.; Iyer, L.; Riccio, E.; Mirsalis, J.; Bathhurst, I.; Rueckle, T.; Ding, X.; Campo, B.; Leroy, D.; Rogers, M. J.; Rathod, P. K.; Burrows, J. N.; Charman, S. A. A long-duration dihydroorotate dehydrogenase inhibitor (DSM265) for prevention and treatment of malaria. *Sci. Transl. Med.* **2015**, *7*, 296ra111.
13. Phillips, M. A.; Rathod, P. K. Plasmodium dihydroorotate dehydrogenase: a promising target for novel anti-malarial chemotherapy. *Infect. Disord.: Drug Targets* **2010**, *10*, 226-39.
14. Phillips, M. A.; Rathod, P. K.; Baldwin, J.; Gujjar, R. Dihydroorotate dehydrogenase inhibitors with selective anti-malarial activity. . *WO Patent 2007149211 A1*, 2007 **2007**.
15. Phillips, M. A.; Gujjar, R.; Malmquist, N. A.; White, J.; El Mazouni, F.; Baldwin, J.; Rathod, P. K. Triazolopyrimidine-based dihydroorotate dehydrogenase inhibitors with potent and selective activity against the malaria parasite, Plasmodium falciparum. *J. Med. Chem.* **2008**, *51*, 3649-3653.
16. Gujjar, R.; Marwaha, A.; El Mazouni, F.; White, J.; White, K. L.; Creason, S.; Shackleford, D. M.; Baldwin, J.; Charman, W. N.; Buckner, F. S.; Charman, S.; Rathod, P. K.; Phillips, M. A. Identification of a metabolically stable triazolopyrimidine-based dihydroorotate dehydrogenase inhibitor with antimalarial activity in mice. *J. Med. Chem.* **2009**, *52*, 1864-1872.

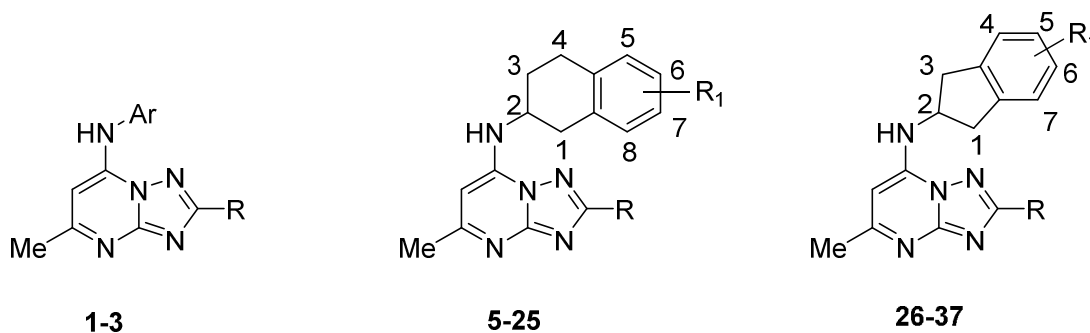
- 1  
2  
3  
4  
5  
6  
7  
8  
9  
10  
11  
12  
13  
14  
15  
16  
17  
18  
19  
20  
21  
22  
23  
24  
25  
26  
27  
28  
29  
30  
31  
32  
33  
34  
35  
36  
37  
38  
39  
40  
41  
42  
43  
44  
45  
46  
47  
48  
49  
50  
51  
52  
53  
54  
55  
56  
57  
58  
59  
60
17. Deng, X.; Gujjar, R.; El Mazouni, F.; Kaminsky, W.; Malmquist, N. A.; Goldsmith, E. J.; Rathod, P. K.; Phillips, M. A. Structural plasticity of malaria dihydroorotate dehydrogenase allows selective binding of diverse chemical scaffolds. *J. Biol. Chem.* **2009**, *284*, 26999-27009.
18. Deng, X.; Kokkonda, S.; El Mazouni, F.; White, J.; Burrows, J. N.; Kaminsky, W.; Charman, S. A.; Matthews, D.; Rathod, P. K.; Phillips, M. A. Fluorine modulates species selectivity in the triazolopyrimidine class of Plasmodium falciparum dihydroorotate dehydrogenase inhibitors. *J. Med. Chem.* **2014**, *57*, 5381-5394.
19. Gujjar, R.; El Mazouni, F.; White, K. L.; White, J.; Creason, S.; Shackelford, D. M.; Deng, X.; Charman, W. N.; Bathurst, I.; Burrows, J.; Floyd, D. M.; Matthews, D.; Buckner, F. S.; Charman, S. A.; Phillips, M. A.; Rathod, P. K. Lead-optimization of aryl and aralkyl amine based triazolopyrimidine inhibitors of Plasmodium falciparum dihydroorotate dehydrogenase with anti-malarial activity in mice. *J. Med. Chem.* **2011**, *54*, 3935-3949.
20. Ganesan, S. M.; Morrissey, J. M.; Ke, H.; Painter, H. J.; Laroia, K.; Phillips, M. A.; Rathod, P. K.; Mather, M. W.; Vaidya, A. B. Yeast dihydroorotate dehydrogenase as a new selectable marker for Plasmodium falciparum transfection. *Mol. Biochem. Parasitol.* **2011**, *177*, 29-34.
21. Ring, B. J.; Chien, J. Y.; Adkison, K. K.; Jones, H. M.; Rowland, M.; Jones, R. D.; Yates, J. W.; Ku, M. S.; Gibson, C. R.; He, H.; Vuppugalla, R.; Marathe, P.; Fischer, V.; Dutta, S.; Sinha, V. K.; Bjornsson, T.; Lave, T.; Poulin, P. PhRMA CPCDC initiative on predictive models of human pharmacokinetics, part 3: Comparative assessment of prediction methods of human clearance. *J. Pharm. Sci.* **2011**, *100*, 4090-4110.
22. Kannankeril, P.; Roden, D. M.; Darbar, D. Drug-induced long QT syndrome. *Pharmacol. Rev.* **2010**, *62*, 760-781.

- 1  
2  
3  
4  
5  
6  
7  
8  
9  
10  
11  
12  
13  
14  
15  
16  
17  
18  
19  
20  
21  
22  
23  
24  
25  
26  
27  
28  
29  
30  
31  
32  
33  
34  
35  
36  
37  
38  
39  
40  
41  
42  
43  
44  
45  
46  
47  
48  
49  
50  
51  
52  
53  
54  
55  
56  
57  
58  
59  
60
23. Jimenez-Diaz, M. B.; Mulet, T.; Viera, S.; Gomez, V.; Garuti, H.; Ibanez, J.; Alvarez-Doval, A.; Shultz, L. D.; Martinez, A.; Gargallo-Viola, D.; Angulo-Barturen, I. Improved murine model of malaria using Plasmodium falciparum competent strains and non-myelodepleted NOD-scid IL2Rgammanull mice engrafted with human erythrocytes. *Antimicrob. Agents Chemother.* **2009**, *53*, 4533-4536.
24. Sirimulla, S.; Bailey, J. B.; Vegesna, R.; Narayan, M. Halogen interactions in protein-ligand complexes: implications of halogen bonding for rational drug design. *J. Chem. Inf. Model.* **2013**, *53*, 2781-2791.
25. Baldwin, J.; Farajallah, A. M.; Malmquist, N. A.; Rathod, P. K.; Phillips, M. A. Malarial dihydroorotate dehydrogenase. Substrate and inhibitor specificity. *J. Biol. Chem.* **2002**, *277*, 41827-41834.
26. Booker, M. L.; Bastos, C. M.; Kramer, M. L.; Barker jr, R. H.; Skerlj, R.; Bir Sdhu, A.; Deng, X.; Celatka, C.; Cortese, J. F.; Guerrero Bravo, J. E.; Krespo Llado, K. N.; Serrano, A. E.; Angulo-Barturen, I.; Belén Jiménez-Díaz, M.; Viera, S.; Garuti, H.; Wittlin, S.; Papastogiannidis, P.; Lin, J.; Janse, C. J.; Khan, S. M.; Duraisingh, M.; Coleman, B.; Goldsmith, E. J.; Phillips, M. A.; Munoz, B.; Wirth, D. F.; Klinger, J. D.; Wiegand, R.; Sybertz, E. Novel inhibitors of Plasmodium falciparum dihydroorotate dehydrogenase with anti-malarial activity in the mouse model. *J. Biol. Chem.* **2010**, *285*, 33054-33064.
27. Bevan, C. D.; Lloyd, R. S. A high-throughput screening method for the determination of aqueous drug solubility using laser nephelometry in microtiter plates. *Anal. Chem.* **2000**, *72*, 1781-1787.

- 1  
2  
3  
4  
5  
6  
7  
8  
9  
10  
11  
12  
13  
14  
15  
16  
17  
18  
19  
20  
21  
22  
23  
24  
25  
26  
27  
28  
29  
30  
31  
32  
33  
34  
35  
36  
37  
38  
39  
40  
41  
42  
43  
44  
45  
46  
47  
48  
49  
50  
51  
52  
53  
54  
55  
56  
57  
58  
59  
60
28. Jantratid, E.; Janssen, N.; Reppas, C.; Dressman, J. B. Dissolution media simulating conditions in the proximal human gastrointestinal tract: an update. *Pharm. Res.* **2008**, *25*, 1663-1676.
29. Nilsen, A.; LaCrue, A. N.; White, K. L.; Forquer, I. P.; Cross, R. M.; Marfurt, J.; Mather, M. W.; Delves, M. J.; Shackelford, D. M.; Saenz, F. E.; Morrisey, J. M.; Steuten, J.; Mutka, T.; Li, Y.; Wirjanata, G.; Ryan, E.; Duffy, S.; Kelly, J. X.; Sebayang, B. F.; Zeeman, A. M.; Noviyanti, R.; Sinden, R. E.; Kocken, C. H.; Price, R. N.; Avery, V. M.; Angulo-Barturen, I.; Jimenez-Diaz, M. B.; Ferrer, S.; Herreros, E.; Sanz, L. M.; Gamo, F. J.; Bathurst, I.; Burrows, J. N.; Siegl, P.; Guy, R. K.; Winter, R. W.; Vaidya, A. B.; Charman, S. A.; Kyle, D. E.; Manetsch, R.; Riscoe, M. K. Quinolone-3-diarylethers: a new class of antimalarial drug. *Sci. Transl. Med.* **2013**, *5*, 177ra37.
30. Bruker. *APEX2* (Version 2.1-4), *SAINT* (version 7.34A), *SADABS* (version 2007/4), BrukerAXS Inc, Madison, Wisconsin, USA. **2007**.
31. Altomare, A.; Burla, C.; Camalli, M.; Cascarano, L.; Giacovazzo, C.; Guagliardi, A.; Moliterni, A.; Polidori, G.; Spagna, R. SIR97: a new tool for crystal structure determination and refinement. *J. Appl. Crystallogr.* **1999**, *32*, 115-119.
32. Altomare, A.; Cascarano, G.; Giacovazzo, C.; Guagliardi, A. Completion and refinement of crystal structures with SIR 92. *J. Appl. Cryst.* **1983**, *26*, 343-350.
33. Mackay, S.; Edwards, C.; Henderson, A.; Gilmore, C.; Stewart, N.; Shankland, K.; Donald, A. *MaXus*: a computer program for the solution and refinement of crystal structures from diffraction data. University of Glasgow, Scotland **1997**.
34. Sheldrick, G. *SHELXL97, Program for the Refinement of Crystal Structures*. University of Gottingen, Germany: 1997.

- 1  
2  
3 35. Waasmaier, D.; Kirfel, A. New analytical scattering-factor functions for free atoms and  
4 ions. *Acta Crystallogr., Sect. A: Found. Crystallogr.* **1995**, *51*, 416-431.  
5  
6  
7  
8 36. Otwinowski, Z.; Minor, W. Processing of X-ray diffraction data collected in oscillation  
9 mode. *Methods Enzymol.* **1997**, *276*, 307-326.  
10  
11  
12 37. McCoy, A. J. Solving structures of protein complexes by molecular replacement with  
13 Phaser. *Acta Crystallogr., Sect. D: Biol. Crystallogr.* **2007**, *63*, 32-41.  
14  
15  
16  
17 38. Emsley, P.; Cowtan, K. Coot: model-building tools for molecular graphics. *Acta*  
18 *Crystallogr., Sect. D: Biol. Crystallogr.* **2004**, *60*, 2126-2132.  
19  
20  
21  
22 39. Adams, P. D.; Afonine, P. V.; Bunkoczi, G.; Chen, V. B.; Davis, I. W.; Echols, N.;  
23 Headd, J. J.; Hung, L. W.; Kapral, G. J.; Grosse-Kunstleve, R. W.; McCoy, A. J.; Moriarty, N.  
24 W.; Oeffner, R.; Read, R. J.; Richardson, D. C.; Richardson, J. S.; Terwilliger, T. C.; Zwart, P.  
25 H. PHENIX: a comprehensive Python-based system for macromolecular structure solution. *Acta*  
26 *Crystallogr., Sect. D: Biol. Crystallogr.* **2010**, *66*, 213-221.  
27  
28  
29  
30  
31  
32  
33  
34  
35  
36  
37  
38  
39  
40  
41  
42  
43  
44  
45  
46  
47  
48  
49  
50  
51  
52  
53  
54  
55  
56  
57  
58  
59  
60

Table 1: Structure–Activity Relationship



Cmpd	R	Ar/R <sub>1</sub>	IC <sub>50</sub> (μM)			EC <sub>50</sub> (μM)
			<i>Pf</i> DHODH	<i>Pv</i> DHODH	<i>h</i> DHODH	<i>Pf</i> βD7 cells <sup>c</sup>
<b>1</b>	CF <sub>2</sub> CH <sub>3</sub>	4-SF <sub>5</sub> -Ph	0.0089 (0.0073 - 0.011)	0.027 (0.023 - 0.032)	>100	0.0043 – 0.0078
<b>2</b>	H	2-Naphthyl	0.047	0.23	>100	0.068
<b>3</b>	H	4-CF <sub>3</sub> -Ph	0.28	2.6	>100	0.34
<b>5</b>	CF <sub>2</sub> CH <sub>3</sub>	H	0.021 (0.019 - 0.024)	0.035 (0.030- 0.041)	ND	0.0028 (0.0022 – 0.0037)
<b>6</b>	CF <sub>2</sub> CH <sub>3</sub>	6-F	0.024 (0.021 - 0.027)	0.056 (0.048 - 0.066)	>100	0.0075 (0.0063-0.0089)
<b>7</b>	CF <sub>2</sub> CH <sub>3</sub>	6-Cl (E-I)	0.0037 (0.0021 - 0.0066)	0.029 (0.019-0.042)	>100	0.0038 (0.0030-0.0049)
<b>8</b>	CF <sub>2</sub> CH <sub>3</sub>	6-Cl (E-II)	1.34 (1.1-1.7)	ND	>100	0.42 (0.37-0.47)
<b>9</b>	CF <sub>2</sub> CH <sub>3</sub>	7-Cl (E-I, <i>S</i> )	0.0063 (0.005 - 0.008)	0.010 (0.0083- 0.013)	>100	0.0012 (0.0011-0.0013)
<b>10</b>	CF <sub>2</sub> CH <sub>3</sub>	7-Cl (E-II, <i>R</i> )	0.79 (0.70-0.94)	ND	>100	2.8 (1.0-7.8)
<b>11</b>	CF <sub>2</sub> CH <sub>3</sub>	6-Br (E-I) <sup>a</sup>	0.0046 (0.0038- 0.0056)	0.024 (0.021 - 0.027)	>100	0.0026 (0.0016 – 0.0042)
<b>12</b>	CF <sub>2</sub> CH <sub>3</sub>	6-Br (E-II) <sup>b</sup>	0.79 (0.59-1.1)	2.1 (1.8-2.5)	>100	0.14 (0.090 – 0.21)
<b>13</b>	CF <sub>2</sub> CH <sub>3</sub>	7-Br (E-I)	0.0046 (0.0036 - 0.006)	0.012 (0.010 - 0.013)	>100	0.00039 (0.00034-0.00044)
<b>14</b>	CF <sub>2</sub> CH <sub>3</sub>	7-Br (E-II)	0.64 (0.53-0.77)	ND	>100	1.4 (1.2-1.5)
<b>15</b>	CF <sub>2</sub> CH <sub>3</sub>	6-OMe	0.14 (0.11-0.16)	0.22 (0.20-0.25)	>100	0.017 (0.014-0.019)
<b>16</b>	CF <sub>2</sub> CH <sub>3</sub>	7-OMe (E-I)	0.021 (0.018-0.024)	0.13 (0.11-0.15)	>100	0.025 (0.023-0.026)
<b>17</b>	CF <sub>2</sub> CH <sub>3</sub>	7-OMe (E-II)	1.0 (0.86 - 1.2)	ND	ND	0.64 (0.56-0.75)

18	CF <sub>2</sub> CH <sub>3</sub>	6,7-di-F (E-I)	2.3 (1.9-2.8)	ND	ND	>2.5
19	CF <sub>2</sub> CH <sub>3</sub>	6,7-di-F (E-II)	0.060 (0.049-0.072)	0.071 (0.066-0.076)	ND	0.022 (0.018-0.026)
20	CF <sub>2</sub> CH <sub>3</sub>	6-F,7- CF <sub>3</sub>	0.089 (0.078-0.10)	0.39 (0.34-0.44)	>100	0.097 (0.080 – 0.12)
21	CF <sub>2</sub> CH <sub>3</sub>	6- CF <sub>3</sub> , 7-F	0.087 (0.067-0.11)	0.82 (0.69-0.96)	>100	3.3 (2.97-3.63)
22	CF <sub>3</sub>	H	0.17 (0.12-0.23)	ND	>100	0.021 (0.017-0.025)
23	CF <sub>3</sub>	6-F	0.077 (0.066 - 0.089)	0.28 0.25-0.33	ND	0.066 (0.062-0.07)
24	CF <sub>3</sub>	7-Cl (E-I)	0.015 (0.012-0.018)	ND	>50	0.033 (0.030-0.035)
25	CF <sub>3</sub>	7-Cl (E-II)	1.1 (0.98-1.2)	ND	ND	1.5 (1.2-1.7)
26	CF <sub>2</sub> CH <sub>3</sub>	H	0.048 (0.040-0.059)	ND	>100	0.036 (0.031 – 0.042)
27	CF <sub>2</sub> CH <sub>3</sub>	5-Br	0.11 (0.083-0.14)	ND	ND	0.59 (0.25-1.4)
28	CF <sub>2</sub> CH <sub>3</sub>	5-Cl	0.085 (0.075-0.097)	ND	ND	0.12 (0.045-0.20)
29	CF <sub>2</sub> CH <sub>3</sub>	5,6-di-Cl	0.14 (0.11-0.17)	ND	ND	0.58 (0.22-1.5)
30	CF <sub>2</sub> CH <sub>3</sub>	5-SO <sub>2</sub> Me	4.0 (2.7-6.1)	ND	ND	6.5 (4.9-8.1)
31	CF <sub>2</sub> CH <sub>3</sub>	5- SO <sub>2</sub> NMe <sub>2</sub>	8.0 (6.7-9.7)	ND	ND	Nd
32	CF <sub>2</sub> CH <sub>3</sub>	4,7-di-Me	0.014 (0.012- 0.017)	0.024 (0.022- 0.027)	>100	0.00039 (0.00021 – 0.00075)
33	CF <sub>2</sub> CH <sub>3</sub>	4,7-di-F	0.065 (0.057-0.075)	0.15 (0.14-0.16)	>100	0.046 (0.002-0.0048)
34	CF <sub>2</sub> CH <sub>3</sub>	4-F	0.052 (0.041-0.066)	0.3 (0.26-0.34)	>100	0.064 (0.061-0.066)
35	CF <sub>2</sub> CH <sub>3</sub>	5,6-di-F	0.052 (0.042-0.064)	0.37 (0.28-0.50)	>100	0.040 (0.035-0.044)
36	CF <sub>2</sub> CH <sub>3</sub>	4-CF <sub>3</sub>	0.066 (0.054- 0.080)	0.28 (0.22 - 0.34)	>100	0.0043 (0.0029-0.0056)
37	CF <sub>3</sub>	5,6-di-F	0.12 (0.11-0.14)	ND	ND	0.15 (0.092-0.23)

DHODH IC<sub>50</sub> and *P. falciparum* EC<sub>50</sub> values were determined from triplicate data points at each concentration in the dose titration. Values in parenthesis represent the 95% confidence interval of the fit.  
<sup>a</sup>Enantiomer-I is the second eluted on the chiral column. <sup>b</sup>Enantiomer-II is the first eluted on the chiral column. <sup>c</sup>Data were collected using albumax unless otherwise stated. Data for **2**<sup>15</sup> and **3**<sup>16</sup> were taken from previous reports reported. **1** has been previously profiled in these assays and parasite data were previously reported.<sup>11, 12</sup> Enzyme data were recollected herein to serve as a direct comparator.

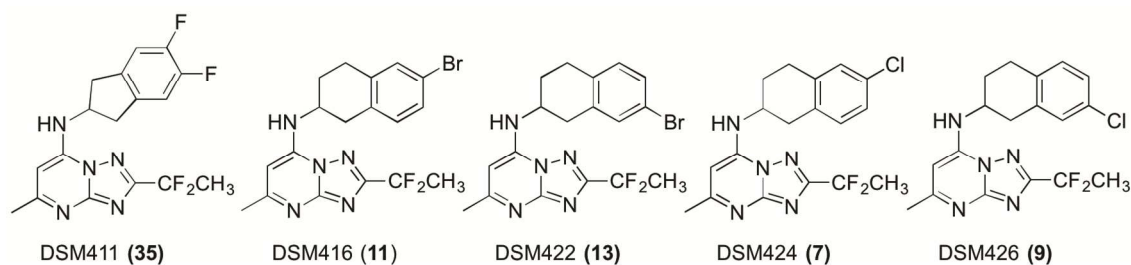


**Table 2. Activity of select triazolopyrimidines on various mammalian DHODHs**

Compound	DHODH IC <sub>50</sub> (μM)			
	human	rat	mouse	dog
<b>1<sup>a</sup></b>	~100	2.6 ± 0.39	2.3 ± 0.64	16 ± 6.5
<b>35</b>	>100	>100	>100	>100
<b>11</b>	>100	>100	>100	>100
<b>13</b>	>100	>100	>100	>100
<b>7</b>	>100	>100	>100	>100
<b>9</b>	>100	>100	>100	>100

<sup>a</sup>errors represent standard deviation for 4 independent replicates using different batches. Each replicate IC<sub>50</sub> was determined from triplicate data points at each concentration in the dose titration.

**Table 3: Physicochemical properties, *in vitro* metabolism and hERG activity.**

Compd	Log D <sub>pH 7.4</sub>	Kinetic solubility pH 6.5 (μg/mL) <sup>a</sup>	PPB <sup>b</sup> (H/R/M, % bound)	Blood to Plasma Ratio (Rat)	<i>In vitro</i> CL <sub>int</sub> (H/R/M, μL/min/mg protein) <sup>c</sup>	Predicted <i>In vivo</i> CL <sub>int</sub> (H/R/M, mL/min/kg) <sup>d</sup>	hERG (μM)
<b>1<sup>e</sup></b>	3.6	12.5-25	99.9/97.7/99.7	0.8	4.3/1.8/2.8	3.5/3.1/7.2	1.6, 6.2
<b>2<sup>e</sup></b>	3.2	12.5-25	ND	ND	96/ND/229	79/ND/591	ND
<b>3<sup>e</sup></b>	2.5	6.3-12.5	ND	ND	7.5/ND/ND	6.2/ND/ND	ND
<b>6</b>	3.5	6.3-12.5	ND	ND	14/39/122	12/67/315	0.7
<b>7</b>	3.9	3.1-6.3	98.8/99.2/ND	0.7	<7/33/44	<5.8/57/114	1.4
<b>9</b>	3.9	3.1-6.3	96.7/96.4/97.4	1.5	<7/38/31	<5.8/65/80	1.5
<b>11</b>	4.0	3.1-6.3	99.0/99.7/99.2	0.7	<7/11/26	<5.8/19/67	0.5
<b>12</b>	4.0	3.1-6.3	ND	ND	<7/13/40	<5.8/22/103	ND
<b>13</b>	4.0	1.6-3.1	96.3/97.2/ND	1.5	<7/39/32	5.8/67/83	1.1
<b>16</b>	3.3	12.5-25	ND	ND	18/19/25	15/33/65	1.8
<b>19</b>	ND	ND	ND	ND	11/24/59	9.1/41/152	ND
<b>20</b>	4.0	3.1-6.3	ND	ND	<7/13/17	<5.8/22/44	ND
<b>21</b>	4.1	1.6-3.1	ND	ND	<7/<7/<7	<5.8/<12/<18	ND
<b>24</b>	4.1	1.6-3.1	ND	ND	9/ND24	7.4/ND/62	ND
<b>26</b>	3.1	25-50	ND	ND	24/245/1004	20/422/2590	ND
<b>28</b>	3.5	6.3-12.5	ND	ND	10/54/43	8.2/93/111	ND
<b>32</b>	3.8	6.3-12.5	ND	ND	168/178/1000	138/306/2580	ND
<b>33</b>	3.2	6.3-12.5	ND	ND	33/1013/1500	27/1740/3870	ND
<b>34</b>	3.3	12.5-25	ND	ND	11/72/76	9.1/124/196	ND
<b>35</b>	3.4	6.3-12.5	93.4/94.2/95.3	1.2	<7/<7/21	<5.8/<12/54	1.7

36	3.7	6.3-12.5	ND	XX	30/61/119	25/105/307	ND
----	-----	----------	----	----	-----------	------------	----

<sup>a</sup> Kinetic solubility range following 30 min at room temperature

<sup>b</sup> Protein binding by ultracentrifugation in human (H), rat (R), and mouse (M) plasma

<sup>c</sup> *In vitro* intrinsic clearance in human (H), rat (R) and mouse (M) liver microsomes

<sup>d</sup> Predicted *in vivo* intrinsic clearance obtained using physiological scaling factors<sup>21</sup>

<sup>e</sup> Values for compounds 1-3 have been previously reported<sup>12, 15, 16</sup>

ND, not determined. c.n.c, could not calculate

Table 4. Solubility in physiologically relevant media<sup>a</sup>

Media	Solubility (µg/ml)					
	1 <sup>b</sup>	35	11	13	7	9
0.1 N HCl	6.8	180	189	52	429	105
FeSSIF pH 5.0	27.6 <sup>c</sup>	65 <sup>c</sup>	211 <sup>c</sup>	39	211	36
FaSSIF pH 6.5	5.1	15	13	8.3	47	12

<sup>a</sup> Solubility after 5-6 h at 37°C; FaSSIF = fasted state simulated intestinal fluid, FeSSIF = fed state simulated intestinal fluid.

<sup>b</sup> Data from <sup>12</sup>

<sup>c</sup> pH 5.8

**Table 5. Inhibition of cytochrome P450 enzymes in human liver microsomes**

<b>CYP</b>	<b>35</b>	<b>11</b>	<b>13</b>	<b>7</b>	<b>9</b>
	<b>IC<sub>50</sub> (μM)</b>				
<b>1A2</b>	>20	>20	>20	>20	>20
<b>2B6</b>	>20	17.7	>20	18.4	>20
<b>2C8</b>	ND	18.7	16.9	>20	>20
<b>2C9</b>	18.5	8.7	3.1	10.2	2.1
<b>2C19</b>	>20	>20	>20	>20	>20
<b>2D6</b>	5.9	>20	3.9	20	2.7
<b>3A4</b>	>20	>20	>20	>20	>20

**Table 6. Mouse plasma pharmacokinetic parameters after a single oral dose. Values in parentheses have been corrected for plasma protein binding and represent unbound values.**

	<b>1<sup>a</sup></b>	<b>35</b>	<b>11</b>	<b>13</b>	<b>7</b>	<b>9</b>
<b>Dose (mg/kg)</b>	10	20	20	20	20	20
<b>Mouse PPB (% bound)</b>	99.7	95.3	99.2	97.2 <sup>b</sup>	99.2 <sup>b</sup>	97.4
<b>T<sub>max</sub> (h)</b>	1.5	1	1	1	1	1
<b>Apparent T<sub>1/2</sub> (h)</b>	2.5	2.3	2.1	2.1	1.9	1.5
<b>C<sub>max</sub> (μM)</b>	3.1 (0.01)	29 (1.4)	8.6 (0.07)	4.5 (0.13) <sup>b</sup>	7.0 (0.06) <sup>b</sup>	5.0 (0.13)
<b>AUC<sub>0-inf</sub> (μM.h)</b>	22.6 (0.07)	169 (7.9)	51 (0.41)	16.7 (0.47) <sup>b</sup>	19.7 (0.16) <sup>b</sup>	22.7 (0.59)

<sup>a</sup> Average from two studies as previously reported<sup>12</sup>.

<sup>b</sup> Protein binding in mouse plasma is an approximation based on rat and human plasma protein binding data. Calculated unbound parameters (in italics) are therefore approximations only.

**Table 7. Rat plasma pharmacokinetic parameters after intravenous (IV) or oral (PO) administration<sup>a</sup>. Values in parentheses have been corrected for plasma protein binding and represent unbound values.**

Intravenous Administration						
Parameter	1 <sup>b</sup>	35	11	13	7	9
Dose (mg/kg)	2.6	1.8	2.0	1.1	1.9	1.6
Rat PPB (% bound)	97.7	94.2	99.7	97.2	99.2	96.4
Blood:Plasma	0.8	1.2	0.7	1.5	0.7	1.5
Apparent T <sub>1/2</sub> (h)	12.6	11.2	6.2	6.1	7.1	5.9
AUC <sub>0-inf</sub> (μM.h)	17.4 (0.40)	27.1 (1.57)	30 (0.09)	2.0 (0.05)	24 (0.19)	3.5 (0.12)
CL <sub>p</sub> (mL/min/kg)	6.0 (263)	3.0 (52)	2.8 (933)	22.4 (800)	3.5 (438)	21.2 (589)
V <sub>ss</sub> (L/kg)	5.9 (257)	2.7 (47)	1.1 (367)	8.7 (311)	1.5 (188)	6.7 (186)
Oral Administration						
Dose (mg/kg)	18.8	21.3	24.4	18.3	18.2	17.5
T <sub>max</sub> (h)	7.0	4.0	2.5	3.3	4.0	3.3
C <sub>max</sub> (μM)	3.9 (0.09)	12.5 (0.72)	37 (0.11)	2.7 (0.07)	23.8 (0.19)	3.3 (0.12)
AUC <sub>0-inf</sub> (μM.h)	122 (2.80)	202 (11.7)	318 (0.95)	28.1 (0.79)	227 (1.82)	24.6 (0.89)
Oral BA (%)	57	63	86	86	100	67

<sup>a</sup>Values represent the average n=2 rats per dose group.

<sup>b</sup>Data from<sup>12</sup>.

Table 8. SCID mouse efficacy data based on once daily (QD) dosing for 4 days<sup>a</sup>

Compound	ED <sub>90</sub> (mg/kg/day)	AUC <sub>ED90</sub> (μM.h /day)
<b>9</b> <sup>b</sup>	~19	10.3
<b>35</b> <sup>b</sup>	~35	~137
<b>7</b> <sup>b</sup>	>30	>23
<b>1 QD</b> <sup>c</sup>	8.1	45.7
<b>1 BID</b> <sup>d</sup>	3.0	30.8
Chloroquine <sup>d</sup>	4.3	3.1

<sup>a</sup> ED<sub>90</sub> was calculated from parasitemia levels measured 24 h after the last dose. AUC data are based on Day 1 pharmacokinetic data.

<sup>b</sup> Based on only two dose levels administered.

<sup>c</sup> **1 QD** data were taken from <sup>11</sup> and converted to different units for consistency.

<sup>d</sup> **1 BID** and chloroquine data were taken from <sup>12</sup> and converted to different units for consistency.

**Figure Legends.**

**Fig. 1.** Structures of selected triazolopyrimidine *Pf*DHODH inhibitors.

The shown structures include, 2-(1,1-Difluoroethyl)-5-methyl-N-[4-(pentafluoro- $\lambda$  6-sulfanyl)phenyl]-[1,2,4]triazolo[1,5-*a*]pyrimidin-7-amine (**1**), (5-Methyl[1,2,4]triazolo[1,5-*a*]pyrimidin-7-yl)naphthalen-2-ylamine (**2**), (5-Methyl[1,2,4]triazolo[1,5-*a*]pyrimidin-7-yl)(4-trifluoromethylphenyl)amine (**3**).

**Fig. 2.** X-ray structure of *Pf*DHODH bound to **13** (*Pf*DHODH-**13**). Limited residues from the 4Å shell around **13** are shown, and the structure has been aligned to the *Pf*DHODH structure bound to **2** (3I65) to allow comparison of the binding modes. Only the inhibitor **2** from 3I65 is displayed. *Pf*DHODH amino acid, FMN and orotate carbons are shown in purple, the carbons of **13** are shown in tan and the carbons of **2** are shown in green. Nitrogens are blue, oxygens are red, sulfur is light yellow, fluorines are light blue, and bromine is deep red. Protein residues are labeled with their amino acid number.

**Fig. 3.** Plasma concentration versus time profiles following a single oral dose of 20 mg/kg to male Swiss outbred mice. Data represent the mean concentrations for two mice at each time point.

**Fig. 4.** Plasma concentration versus time profiles following a single intravenous (IV) or oral (PO) dose to male Sprague Dawley rats. Dose levels are shown in Table 7. Each data point represents the mean of data from two rats and error bars represent the range.

**Fig. 5.** SCID mouse *in vivo* efficacy data. Mice were infected with *P. falciparum* Pf3D7<sub>0087/N9</sub> parasites by intravenous injection on day zero and dosing was once daily for four days starting on day 3 post infection. A. Blood parasitemia levels were monitored daily by flow cytometry. B.

1  
2  
3 Pharmacokinetic analysis was performed after the first dose. Pharmacokinetic parameters are  
4  
5 reported in Table S4.  
6  
7  
8  
9  
10  
11  
12  
13  
14  
15  
16  
17  
18  
19  
20  
21  
22  
23  
24  
25  
26  
27  
28  
29  
30  
31  
32  
33  
34  
35  
36  
37  
38  
39  
40  
41  
42  
43  
44  
45  
46  
47  
48  
49  
50  
51  
52  
53  
54  
55  
56  
57  
58  
59  
60

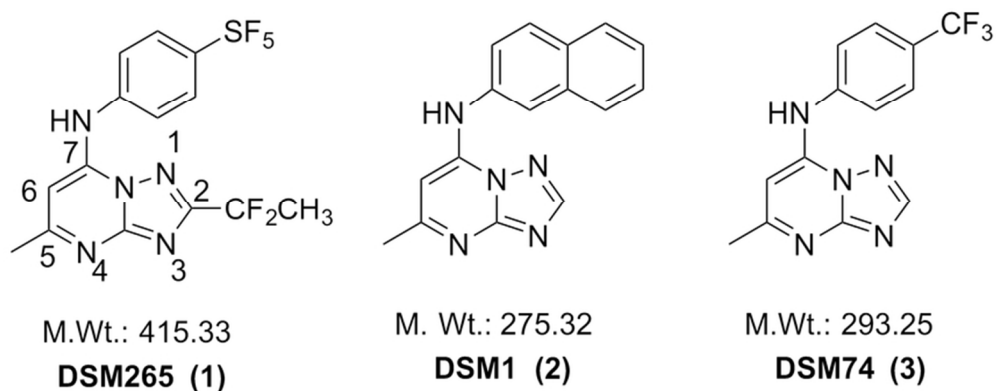


Figure 1  
36x14mm (600 x 600 DPI)

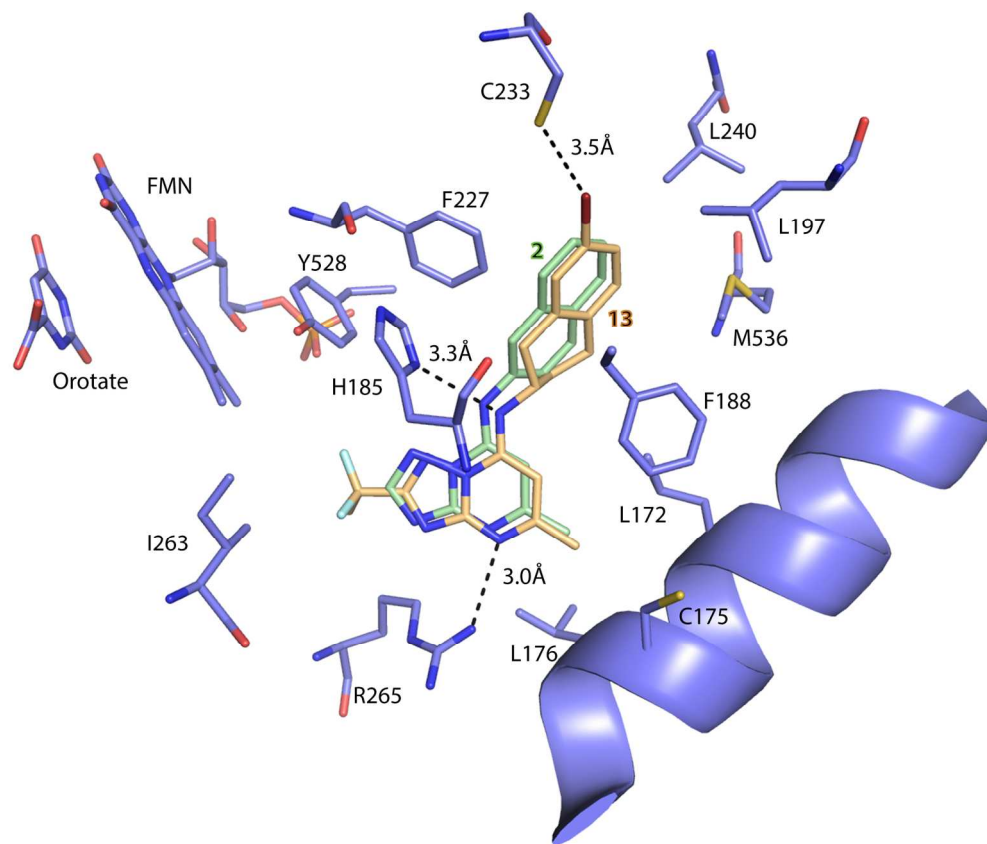


Figure 2  
152x128mm (300 x 300 DPI)

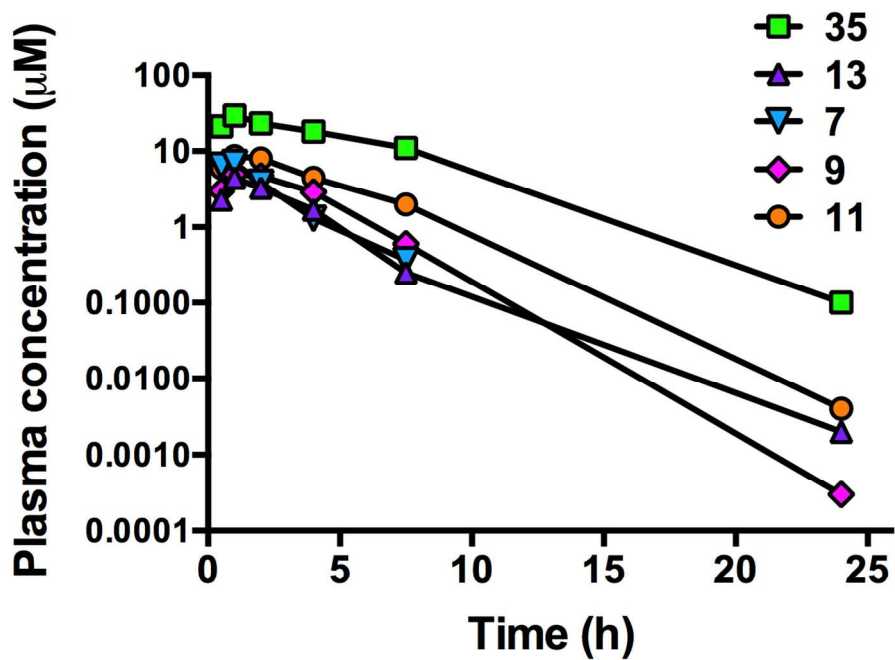


Figure 3  
125x85mm (300 x 300 DPI)

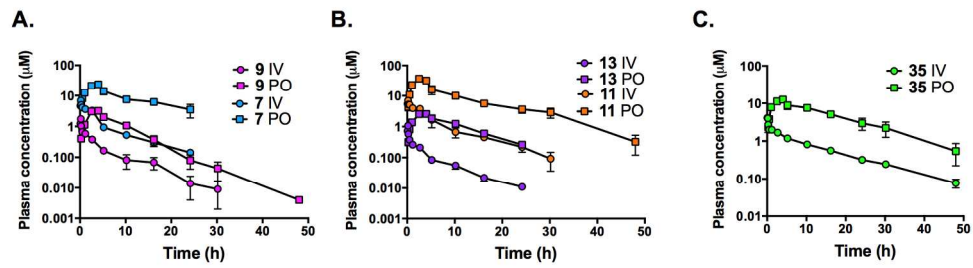


Figure 4  
189x52mm (300 x 300 DPI)

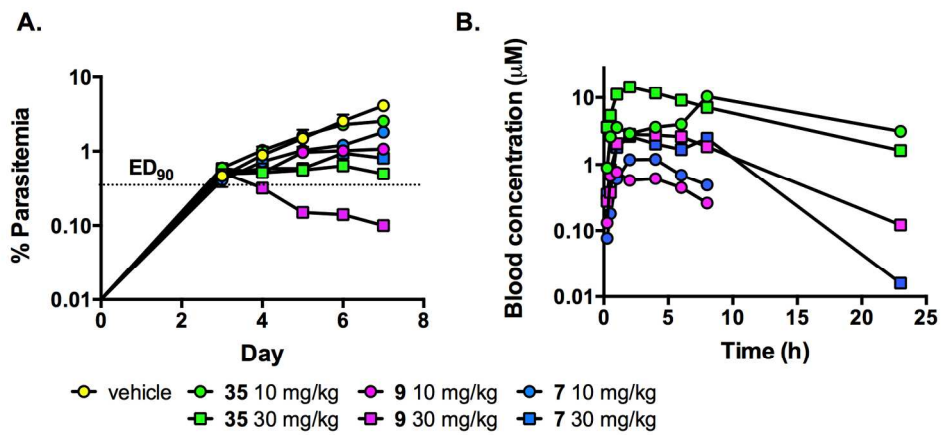


Figure 5  
169x76mm (300 x 300 DPI)

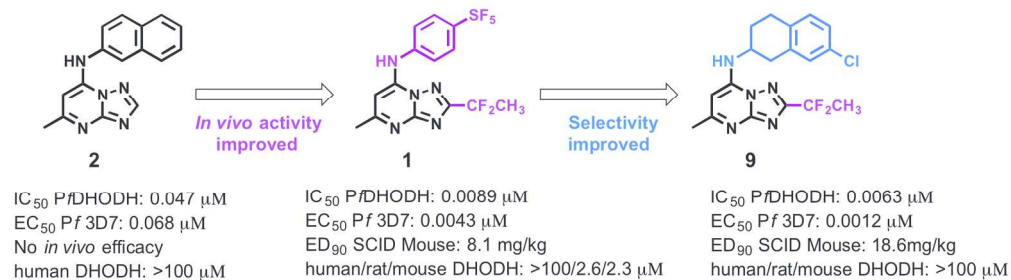


Table of contents graphic  
174x49mm (300 x 300 DPI)